



HAL
open science

Land-use intensity influences European tetrapod food webs

Christophe Botella, Pierre Gaüzère, Louise O'Connor, Marc Ohlmann, Julien Renaud, Yue Dou, Catherine Graham, Peter Verburg, Luigi Maiorano, Wilfried Thuiller

► **To cite this version:**

Christophe Botella, Pierre Gaüzère, Louise O'Connor, Marc Ohlmann, Julien Renaud, et al.. Land-use intensity influences European tetrapod food webs. *Global Change Biology*, 2024, 30 (2), 10.1111/gcb.17167 . hal-04757075

HAL Id: hal-04757075

<https://hal.science/hal-04757075v1>

Submitted on 28 Oct 2024

HAL is a multi-disciplinary open access archive for the deposit and dissemination of scientific research documents, whether they are published or not. The documents may come from teaching and research institutions in France or abroad, or from public or private research centers.

L'archive ouverte pluridisciplinaire **HAL**, est destinée au dépôt et à la diffusion de documents scientifiques de niveau recherche, publiés ou non, émanant des établissements d'enseignement et de recherche français ou étrangers, des laboratoires publics ou privés.

Land-use intensity influences European vertebrate food-webs

Christophe Botella* (christophe.botella@gmail.com)^{1,2}, Pierre Gaüzère (pierre.gauzere@gmail.com)¹, Louise O'Connor (louise.mj.oconnor@gmail.com)¹, Marc Ohlmann (marcohlmann@live.fr)¹ †, Julien Renaud (julien.renaud@univ-grenoble-alpes.fr)¹, Yue Dou (yue.dou@utwente.nl)^{3,4}, Catherine H. Graham⁵, Peter H. Verburg (p.h.verburg@vu.nl)^{4,5}, Luigi Maiorano (luigi.maiorano@uniroma1.it)⁶, Wilfried Thuiller (wilfried.thuiller@univ-grenoble-alpes.fr)¹

¹ Univ. Grenoble Alpes, Univ. Savoie Mont Blanc, CNRS, LECA, F-38000 Grenoble, France

² Centre for Invasion Biology, Department of Botany and Zoology, Stellenbosch University, Stellenbosch, South Africa

³ Department of Natural Resources, Faculty of Geo-information Science and Earth Observation (ITC), University of Twente, Enschede, the Netherlands

⁴ Institute for Environmental Studies, VU University Amsterdam, the Netherlands

⁵ Swiss Federal Research Institute WSL, Birmensdorf, Switzerland

⁶ Department of Biology and Biotechnologies "Charles Darwin", Sapienza University of Rome, Roma, Italy

† Deceased before publication (17/06/2023)

* Corresponding author (tel: +33670970981)

Statement of authorship: CB, PG, LO and WT conceptualised the study. CB, JR, YD, LM and PV collected and preprocessed the data. CB developed the code and analysis. CB, PG, MO and JR made the Figures. All authors validated the results. CB wrote the first draft together with WT. All authors read and reviewed the manuscript.

Data accessibility statement: The data used in this study are available at

<https://zenodo.org/record/7741947>, and the R scripts to reproduce figures and results are provided at

https://github.com/ChrisBotella/foodwebs_vs_land_use.

Funding statement: This study has received funding from the ERA-Net BiodivERsA—Belmont Forum, with the national funder Agence Nationale de la Recherche (ANR-18-EBI4-0009), The Dutch Research Council NWO (grant E10005), and the Swiss National Science Foundation (20BD21_184131/1), part of the 2018 Joint call BiodivERsA-Belmont Forum call (project 'FutureWeb'). WT, JR, LOC, LM and PHV also acknowledge support from the European Union's Horizon Europe under grant agreement number 101060429 (project NaturaConnect). CB was funded by the French Agence Nationale de la Recherche (ANR) through the EcoNet (ANR-18-CE02-0010) project. WT acknowledges support from MIAI@Grenoble Alpes (ANR-19-P3IA-0003) and FORBIC (ANR-18-MPGA-0004). CG also acknowledges funding from the European Research Council (ERC) under the European Union's Horizon 2020 research and innovation program (grant 787638).

Number of words: 149 words in abstract, 5172 words in main text. **5 Figures and 1 Table** in main text.

Number of references: 58. **Running title:** Intensification impacts food-web architecture. **Type of article:** Letter.

Keywords: Trophic networks; food-webs; anthropization; land use ; intensification ; tetrapods ; biotic homogenization; crowdsourcing

42 **Abstract**

43 Land use intensification favours particular trophic groups which can induce architectural
44 changes in food-webs. These changes can impact ecosystem functioning and stability.
45 However, the imprint of land management intensity on food-web architecture has rarely been
46 characterised across large spatial extent and various land uses. We investigated the influence
47 of land management intensity on six facets of food-web architecture for 67,051 European
48 terrestrial vertebrate communities and its dependency on land use and climate. We found that,
49 in general, intensification tended to lower proportions of both apex and basal species, favoured
50 mesopredators and decreased food-webs compartmentalisation. These general trends were
51 particularly strong in forests and settlements, but some contexts, like Mediterranean forest or
52 Atlantic croplands, showed strong and discrepant responses. By favouring mesopredators in
53 most contexts, intensification could undermine basal tetrapods, the cascading effects of which
54 need to be assessed. Our results support apex predator diversity protection where possible.

55

56

57

58

59

60

61

62

63

64

65 **Introduction**

66 Land use intensification and change have been identified as the most impactful factors of
67 biodiversity loss in terrestrial and freshwater ecosystems (Diaz et al., 2019), generating habitat
68 fragmentation or loss (Fahrig et al., 2003), introduction of invasive species (Doherty et al.,
69 2016), direct interactions between humans and wildlife (e.g. exploitation, hunting) and pollution.
70 Increasingly, studies have shown that land use intensification leads to changes in species
71 composition across trophic groups (Gossner et al., 2016, Etard et al., 2022). However, species
72 are not independent of each other. Instead they interact in complex food-webs that reflect the
73 flow of energy and biomass in the system, and the interdependency among species (Link et al.,
74 2005). The architecture of food-webs, namely the configuration of trophic interactions between
75 species in a community, can be summarised into key properties that have an impact on food-
76 web dynamics (e.g. degree of omnivory, generalism, compartmentalization, trophic chain
77 lengths, see Botella et al., 2022). Changes in food-web architecture following land use
78 intensification might be indicative of the potential for ecosystem collapse (Evans et al., 2013,
79 Keyes et al., 2021, Saint-Béat et al., 2015). Food-webs sustain a number of ecosystem
80 functions and services, such as pest control (Montoya et al., 2003), seed dispersal (Corlett,
81 2017), or nutriment cycling in soils (De Vries et al., 2013), and their architecture partly
82 determines community stability (Tylianakis et al., 2010, Saint-Béat et al., 2015, Mestre et al.,
83 2022). We thus urgently need to understand how changes in land use will modify the
84 architecture of food-webs (Li et al., 2018, Rigal et al., 2021). While local studies focusing on
85 specific land uses or taxonomic groups can help formulate hypotheses on how land
86 management intensity affects food-web architecture (Agostini et al., 2020, De Visser et al.,
87 2011, Gossner et al., 2016, Hallmann et al., 2014, Heger et al., 2018, Herbst et al., 2013), we
88 lack a macroecological assessment of these hypotheses and their context-dependence.

89 Local-scale studies have shown that land use intensification favours a limited set of
90 synanthropic and generalist species, in terms of habitat (Clavel et al., 2011) and trophic
91 interactions (McKinney & Lockwood, 1999), at the expense of more specialist ones, leading to
92 biotic homogenization (Gossner et al., 2016, McKinney & Lockwood, 1999). On one hand,
93 intensive grassland management reduces plant diversity and induces local extinction cascades
94 in higher trophic levels (Herbst et al., 2013). Likewise, increased use of pesticides indirectly
95 affect species feeding on plants or invertebrates and is a well-known cause of the loss of basal
96 vertebrate species, such as ~~in~~birds (Geiger et al., 2010, Hallmann et al., 2014) and amphibians
97 (Agostini et al., 2020, Sparling et al., 2001). On the other hand, human activities and habitat loss
98 often negatively affect top predators even more drastically than lower trophic levels (Dobson et
99 al., 2006, Visser et al., 2011, Estes et al., 2011). This might lead to a loss of top-down control of
100 mesopredators in trophic communities, called mesopredator release (Prugh et al., 2009), and
101 offer opportunities for new mesopredators to establish (Heger et al., 2018). The mesopredator
102 release could indirectly generate negative pressure on basal species (Estes et al., 2011). The
103 decrease in richness of both basal species and top predators could induce shorter trophic
104 chains and denser networks through replacement of specialists by generalists or omnivores.
105 These more frequent generalists and omnivores should also make networks less
106 compartmentalised (i.e. groups of species interacting more together than with others are
107 expected to be more rare). These ecological processes related to intensification should thus
108 translate into the following changes on six different facets of food-web architecture (**Figure 1**)
109 that we test here: decreased proportions of (1) apex and (2) basal species, higher proportions of
110 (3) trophic generalists and (4) omnivores, (5) shorter trophic chains and (6) decreased
111 compartmentalization.

112 We build on a recent macro-scale study on European terrestrial vertebrate food-web
113 architectures (Braga et al., 2019) that found a decreased connectance and increased

114 compartmentalization in landscapes more strongly influenced by humans. These trends
115 contradict our general expectations, motivating further investigations accounting for context-
116 dependency. We used a recent high resolution classification of land management intensity for
117 different land uses (Dou et al., 2021), along with massive presence-only observations collected
118 across Europe (GBIF, iNaturalist) and knowledge of trophic interactions between all European
119 terrestrial vertebrates, hereafter called the metaweb (Maiorano et al., 2020). Through a
120 thorough spatial sampling analysis, we reconstructed 67,051 local meta food-webs containing
121 all potential interactions among the species present in a 1km² resolution. These local meta food-
122 webs had a total of 756 vertebrate species and spanned five bioclimatic regions (Atlantic,
123 Continental, Mediterranean, Alpine or Boreal) and six land uses (forest, grasslands, arable and
124 permanent croplands, agricultural mosaics or human settlements) across Europe. We quantified
125 the six above-mentioned architectural facets (**Figure 1**) in each local meta food-web, and
126 evaluated how they were influenced by land management intensity. To investigate the context-
127 dependence of the response to intensification, we tested this response per land use and
128 bioclimatic region.

129 **Material and methods**

130 **Data**

131 **Species presence/absence/uncertainty rasters.** To quantify the effects of land management
132 intensity on European tetrapods trophic networks, we gridded species occurrences from GBIF
133 and iNaturalist. We chose to use these occurrences to complement the extent of occurrence
134 from IUCN or BirdLife, commonly used previously (e.g. Braga et al., 2019, O'Connor et al.,
135 2020), which can not be interpreted as an area of certain presence at our resolution. We
136 considered 756 terrestrial vertebrate (hereafter vertebrate) species with at least one geolocated
137 occurrence after data cleaning (see **Appendix S1**) across continental Europe (35 countries).

138 Since most data in GBIF and iNaturalist are presence-only data, we sub-selected cells to
139 minimise the impact of false absences. More specifically, for each species, we built a raster
140 indicating the presence, absence or uncertain status of that species in each 1km by 1km cell of
141 the land use raster described below (as shown in box 2 of **Figure S1.1**). As a conservative
142 strategy, we first considered a species as absent in a cell if it was out of the species' distribution
143 range provided by the IUCN Red List, including both native and invasive ranges (IUCN, 2021).
144 Within the IUCN range, cells having at least one occurrence of the focal species were
145 considered as presences. The remaining cells for that species (inside the IUCN range but
146 without occurrence) were considered as absences if the sampling effort in the cell exceeded a
147 defined species-specific threshold, or uncertain otherwise. The sampling effort in a cell for a
148 given species was approximated by the total number of occurrences across all species of the
149 same taxonomic class (Aves, Mammalia, Amphibia or Reptilia). The sampling effort threshold to
150 consider this species as absent when undetected was defined as the first decile of sampling
151 effort values across all presence cells of that species. The sensitivity of our main results to the
152 stringency of the sampling effort threshold and taxonomic sampling bias (e.g. favouring Aves
153 compared to Reptilia/Amphibia) were investigated in **Appendix S11**. We excluded from the
154 study all cells where more than 30% of all 756 species (i.e. 227 species) had uncertain status or
155 the observed richness was lower than 20 (box 3 of **Figure S1.1**), because a lower richness is
156 rare in tetrapod communities studied at comparable scale (Braga et al., 2019, Gaüzere et al.,
157 2022) and would likely be due to imperfect detection.

158 After this filtering process, cells were grouped per combination of bioclimatic region and land
159 use (explained further below) only retaining combinations containing enough cells to compare
160 land management intensity levels (see box 4 of **Figure S1.1** for more detail). After cell filtering,
161 we retained 67,051 cells which are summarised by bioclimatic region, land use and
162 management intensity in **Figure S3.4**.

163 **Metaweb of tetrapod trophic interactions.** We used the metaweb of potential trophic
164 interactions between European tetrapod species (Maiorano et al., 2020), which we restricted to
165 756 selected species with enough observations. The metaweb of these species is fully
166 represented in **Figure S2.2** of the Appendix, highlighting its decomposition into 46 trophic
167 groups (the same as in O'Connor et al., 2020); we also provide a simplified visualisation in
168 **Figure 2** where species were aggregated per trophic group.

169 **Local meta food-webs.** The metaweb was used to reconstruct what we call here the local meta
170 food-web associated with the set of species present in each retained cell. Two species were
171 assumed to interact locally if they are both observed in the cell and if they are known to interact
172 in the metaweb. This representation of food-webs can be also seen as a local realisation of the
173 metaweb interactions based on trusted species presences and absences, consistently with
174 many related studies (e.g., Poisot et al., 2012, Kortsch et al., 2019, Braga et al., 2019, O'Connor
175 et al., 2020). Species having locally no prey and predator were kept, as they can feed on non-
176 tetrapod species (aquatic vertebrates, invertebrates, fungi, plants), without affecting most
177 network metrics (see architecture facets' section below).

178 **Land use and management intensity.** We used a new land system map that integrates
179 various land use and land cover data with intensity of use for Europe at 1km² resolution (Dou et
180 al., 2021), which covers EU28+ (including the EU, the United Kingdom, Norway, Switzerland,
181 and the Western Balkans, but excluding Iceland, Turkey and Macaronesia). We considered six
182 land uses: forest, grassland (except grass wetlands), permanent cropland (vineyards, olive
183 groves, fruit gardens), arable cropland, agricultural mosaic (cropland and grassland) and human
184 settlement (cities and peri-urban landscapes). Dou et al. (2021) decomposed each land use into
185 different levels of land management intensity (low/high for permanent croplands,
186 low/medium/high for others) based on criteria that (i) depend on the land use (see **Table S3.2**)

187 and (ii) have documented impacts on biodiversity, which make these land use classifications
188 suitable to our purpose.

189 **Bioclimatic regions.** As climate influences tetrapod food-webs (Braga et al., 2019), we
190 integrated it to control for the influence of its spatial variations in our analysis. We considered
191 the biogeographical regions defined by the European Environment Agency (European
192 Environmental Agency, EEA 2021). These bioclimatic regions represent large scale biodiversity
193 units reflecting climatic contrasts and are based on an interpretation of geobotanical data.
194 Among the 11 original regions, 5 were used in our study, the Alpine, Atlantic, Boreal,
195 Continental and Mediterranean regions, for which we had enough sampled cells (**Figure S3.4**).

196 **Analysis methods**

197 To evaluate the effect of land management intensity on six facets of food-web architecture (see
198 **Figure 1**), we selected one or several network metrics summarising each facet. We measured
199 the mean deviation per metric related to an increase of land management intensity (**Figure 4**)
200 and tested, for each facet, the statistical significance of the multivariate deviation between
201 intensity levels per combination of bioclimatic region and land use (which we refer to as context
202 below, for instance mediterranean forests).

203 **Network architecture facets**

204 The network metrics composing each architecture facet are summarised in **Table 1**. They were
205 computed for each local meta food-web. Detailed explanations are presented in the Appendix
206 **S4**. For apex proportion, we computed the proportion of observed species that are apex
207 predators (**pApexMeta**), which is determined from species trophic levels (MacKay et al., 2020)
208 in the metaweb completed by species diets as additional nodes (as recommended in Maiorano
209 et al., 2020). Diets were represented along with tetrapod trophic groups in the full metaweb

210 visualisation of **Figure 2**. For basal proportions, we computed two metrics: **pBasalMeta** and
211 **pBasal** are the proportion of observed species having no tetrapod prey in the metaweb or local
212 meta food-web, respectively. Both versions of the metric were considered because some of a
213 species' potential prey (metaweb) might have not been detected in local meta food-webs. For
214 connectance, we computed the density of directed trophic interactions among tetrapod species
215 in a local meta food-web (**dirCon**). For omnivory levels, we computed two metrics based on a
216 continuous or categorical view of trophic levels: **omniLvl** is the average, over non-basal and
217 non-apex species in the metaweb, of the standard deviation of their prey's trophic levels, while
218 **omniProp** is the proportion of non-basal and non-apex species in the metaweb predating
219 several levels (basal / intermediary / apex, see Appendix **S4**). For chain indices, we computed
220 the longest (**maxPath**), mean (**meanPath**) and standard deviation (**sdPath**) of the shortest-
221 paths from locally basal species to top species. Finally, for compartmentalization, we computed
222 the local modularity (**modul**, Newman et al., 2006), and the mean distance (**meanShortDist**)
223 between species on the (undirected) local meta food-web. Several metrics were chosen for one
224 facet when one dimension alone could not capture the ecological meaning well. As a logical
225 consequence, metrics inside each facet were positively correlated but weakly correlated
226 between facets (see **Figure S5.6**). We later interpret land management intensity as influencing
227 a given facet only if all its metrics were influenced in the same way.

228 **Mean metric deviations related to land management intensity**

229 To assess the influence of land management intensity on architecture facets and its context-
230 dependence, we measured the mean deviation of each metric related to an increase in land
231 management intensity per context. We fitted a multivariate linear regression (Johnson &
232 Wichern, 1992) over local meta food-webs where the metrics were set as dependent variables,
233 and the combination of context and land management intensity as categorical explanatory
234 variable with nested contrasts, so that the deviation related to a higher intensity level (high or

235 medium compared to low) is nested per context (i.e. estimated for each context). More
236 precisely, these nested contrasts are implemented with the R formula: $\text{metric} \sim \text{bioclimatic}$
237 $\text{region} / \text{land use} / \text{intensity}$). We obtained one mean deviation related to an increase of intensity
238 (high versus low, or mid versus low) for each network metric and for each context (bioclimate
239 and land use). Some combinations were not considered due to a lack of well sampled cells (see
240 **Figure S3.4**). We obtained 38 mean deviations per metric, including deviations from low to
241 medium intensity cells for 20 contexts, and from low to high intensity for 18 contexts, spanning a
242 total of 21 contexts (see Tables **S6.7 to S6.12**, where each table shows one facet). We also
243 tested the robustness of these general results to several potential biases, namely the choice of
244 our sampling effort threshold for species detection, taxonomic detection bias and outlier food-
245 webs, in Appendix **S10**.

246 **Tests of multivariate deviation significance**

247 We tested whether the mean deviations related to an increase of intensity were significant for
248 each facet and context. We tested the equality between the two multivariate distributions of
249 food-web metrics (high versus low intensity, or medium versus low intensity) included in the
250 facet, and detected significant deviations when the null hypothesis was rejected (i.e. no effect
251 of higher land management intensity). This was done using a non-parametric multivariate test
252 based on Wilk's Lambda statistics, which accounts for the unbalanced number of cells between
253 intensity levels (Liu et al., 2011, implemented in the *npmv* R package, Burchett et al., 2017). We
254 defined the risk of detecting at least one false non-equality across our six facets to 5% per
255 context, as explained in **Appendix S6**. The significance of the deviation in each context is
256 indicated by a blue background of cells in Tables **S6.7 to S6.11**.

257 **Results**

258 The influence of land management intensity was overall weaker than those of climate and land
259 use but accounting for land management intensity yielded a greater explanatory power of food-
260 web variability based on the model partial R^2 s (**Table S7.3**). The general influence of land
261 management intensity was quite strongly negative for apex proportions, with a mean relative
262 deviation below -10% (**Figure 4-top**), and substantial on all other facets (around +/-5%), except
263 omnivory, as explained below per facet.

264 **Apex predator proportion decreased strongly under higher land management intensity.** In
265 agreement with our hypothesis, apex predator proportion (p_{ApexMeta}) decreased with
266 increasing land management intensity and had the strongest mean deviation of all food-web
267 metrics (greater than 10% of the interquartile range, **Figure 4-top**). In other words, the decrease
268 of apex proportion in high land use intensity compared to low intensity represents >10% of the
269 inter-quartile range of the overall metric variation among the 70 thousand local meta food-webs
270 when correcting for the effect of climate and land use. This trend was robust with a nearly
271 constant magnitude across sensitivity analyses (**Appendix S10**). This decrease concerned 8 of
272 the 9 highest trophic groups which included only apex predators (**Figure 5**). Negative deviations
273 spanned 15 of the 21 contexts, represented 68% of all deviations, while positive deviations were
274 mostly small (**Figure 4-bottom** and **Figure S6.7**).

275 **Basal species proportions decreased under higher land management intensity.** In
276 agreement with our hypothesis, the two metrics of basal species proportions were lower, with a
277 relative deviation -5% in the most intensively managed landscapes averaging over both metrics
278 (**Figure 4-top**) while controlling for context. This trend was also robust in all sensitivity analyses
279 (**Appendix S10**). These decreases included 12 of the 16 trophic groups containing basal species
280 (**Figure 5**). Fifty percent of the 34 significant mean deviations showed a decrease of both
281 p_{Basal} and $p_{\text{BasalMeta}}$ metrics, spanning half of the 21 contexts (**Figure 4-bottom**, Table 3).
282 This decrease was particularly strong in continental and boreal contexts (**Figure S6.13**).

283 Contrary to our expectation, pBasal and pBasalMeta increased with land management intensity
284 in 26.5% of the significant contexts (**Figure S6.13 and Figure S6.8**).

285 **Connectance substantially increased under higher land management intensity.**

286 Connectance substantially increased in general with land management intensity with a relative
287 deviation greater than +5% (**Figure 4-top**). Positive mean deviations spanned 17 of the 21
288 contexts, represented 74% of all deviations, and were notably strong in all forests except the
289 Mediterranean ones (**Figure S6.9**). Mediterranean contexts hosted most significant negative
290 mean deviations. However, when considering only the most sampled cells for all taxonomic
291 classes, the influence of a higher land management intensity on connectance was negative
292 (**Appendix S10, Figure S11.17**), due to the selection of Spanish Mediterranean cells.

293 **Omnivory showed contrasted responses to land management intensity.** OmniLev and
294 omniProp had context-dependent responses to land management intensity (**Figure 4-top**)
295 across bioclimates and land uses. While most mean deviations were significant (34/38), only
296 23.5% of them showed an increase of both omnivory levels (**Figure 4-bottom**), challenging our
297 expectations. These spanned 6 contexts, including three forest contexts where strong
298 deviations of both metrics were observed under the highest intensity level (**Figure S6.10**). In
299 contrast, omnivory levels both decreased in 47.1% of the significant mean deviations, including
300 all settlement contexts where deviations were particularly strong. These unexpected negative
301 responses might be partly due to the taxonomic sampling bias because both metric mean
302 deviations became positive and increased in magnitude when minimizing this bias in a
303 complementary analysis (**Appendix S10, Figure S11.17**).

304 **Trophic chain lengths increased under high land management intensity in human**

305 **settlements.** Contrary to our expectations, the three metrics describing trophic chain length
306 increased on average with land management intensity but with a moderate magnitude, i.e. the

307 relative deviations were inferior to +10% for the three metrics (**Figure 4-top**). Local meta food-
308 webs under low land management intensity had relatively more shortest-paths of length 1 (direct
309 predation on a basal species), while local meta food-webs under high land management
310 intensity had more shortest-paths of length 2 to 5 (see **Figure S8.13**). This general trend
311 concealed a strong context dependence. Indeed, four out of the nine contexts where we
312 measured significant positive deviations were in human settlements and the relative deviations
313 were strong for the Boreal, Continental and Atlantic settlements (**Figure S6.11**). Outside cities,
314 significant positive deviations covered fewer contexts than significant negative deviations (5
315 versus 6). Besides, the general increase of the three metrics was softer with a more stringent
316 sampling effort quantile for cell selection (**Figure S11.16**) or when removing outlier food-webs
317 (**Figure S11.20**).

318 **Compartmentalization overall decreased under high land management intensity.** Both
319 compartmentalization metrics decreased in general with increasing land management intensity
320 with a moderate magnitude as relative deviations were superior to -10% for both metrics
321 (**Figure 4-top**). This general trend is confirmed by a higher proportion of disconnected pairs of
322 basal and apex species in low intensity food-webs compared to the high intensity ones (**Figure**
323 **S7.12**), i.e. more frequent disconnected trophic chains or species. The decrease was robust in
324 all sensitivity analyses and larger in magnitude for both metrics when correcting for taxonomic
325 bias or removing outlier food-webs (Appendix S10). Of the 34 significant mean deviations, 56%
326 showed a decrease and 27% an increase in both metrics, half of which were located in the
327 Mediterranean region (see **Figure S6.12**).

328 **The influence of land management intensity was strongly context-dependent.** The general
329 influence of land management intensity concealed larger, contrasting effects across different
330 climatic and land-use contexts, as shown by the very spread out relative deviations per
331 contexts, often greater than 20% in absolute value, for all facets (**Figure 4-top**). The sign of

332 mean deviations varied across land uses and bioclimatic regions for all facets, except for apex
333 proportions whose relative deviation was rarely positive and weak in these contexts (lower than
334 +10%). Forests, croplands and settlements showed particularly strong responses in comparison
335 to agricultural mosaic and grasslands: The labels are often further from the centre in **Figure**
336 **S6.13** for forest and settlements contexts. The response of Mediterranean food-webs diverged
337 from the general trends described above and was quite consistent among forest, settlements
338 and croplands of this region: Connectance strongly and significantly decreased while
339 compartmentalization strongly and significantly increased when land management was more
340 intense (illustrated in **Figure S6.13**, detailed deviations in **Figures S6.9, and S6.12**).

341 Mediterranean forests and settlements also showed strongly and significantly increased basal
342 proportions, contrary to most other contexts including Mediterranean croplands (**Figure S6.8**).
343 Even though other settlement contexts followed the general trends, Alpine and Mediterranean
344 settlements strongly differed from it regarding connectance, with a strongly negative deviation
345 (**Figures 6 and S6.9**). The influence of intensification was most opposed to the general trends
346 in Mediterranean forests and Atlantic croplands (**Figure S6.13**), as both contexts showed a
347 sharp increase of basal proportions (**Figure S6.8**), compartmentalization (**Figure S6.11**), and a
348 strong decrease of connectance (**Figure S6.9**) and chain indices (**Figure S6.10**).

349 **Discussion**

350 We demonstrated that, in addition to more commonly considered climatic factors (Braga et al.,
351 2019, Kortsch et al., 2019), the architecture of local meta food-webs is significantly influenced
352 by land use and management intensity. Although the overall impact of land management
353 intensity was less pronounced compared to climate and land use, it still exerted a notable
354 influence on specific trophic groups. Land management intensity generally strongly reduced the
355 proportion of top predators. Furthermore, we observed a substantial negative general influence
356 of intensification on basal tetrapods and compartmentalization, along with a positive influence

357 on connectance and the trophic chain lengths. However, for these latter architecture facets, the
358 influence of intensification was highly contingent on the context. Notably, intensification sharply
359 decreased connectance in Mediterranean and Alpine settlements, and it increased basal
360 proportions and compartmentalisation in Mediterranean forests and Atlantic croplands. Besides,
361 we observed a sharp decrease of omnivory in all settlement contexts.

362 Less intensively used landscapes tend to host local meta food-webs made of a higher
363 proportion of apex and basal tetrapod species and with a greater compartmentalization. This
364 combination of properties strongly suggests that food-webs became topologically more
365 hierarchical (Clauset et al., 2008, see network on left of Figure 1 as an illustration) in response
366 to intensification, namely networks that are similar to a tree. These findings support those of
367 Mestre et al. (2022), who showed that low human pressures favours scale-free architectures,
368 i.e. where the node degree distribution follows a power-law. A scale-free architecture combined
369 with a high compartmentalization results in a hierarchical architecture (Barabási et al., 2003).
370 This hierarchical architecture tends to limit the number of predators per basal species. Apex
371 predators were also relatively more diverse under lower human pressures, suggesting a better
372 regulation of mesopredators, which might indirectly limit the predation pressure on the basal
373 layer (Prugh et al., 2009).

374 High land management intensity resulted in a concentration of species diversity among
375 mesopredators. In these environments, food webs exhibited a reduced proportion of apex
376 predator species, a phenomenon often attributed to direct human interference (Prugh et al.,
377 2009, De Visser et al., 2011, Estes et al., 2011). Additionally, human activities led to a decline in
378 the proportion of basal tetrapod species. Consequently, the proportion of mesopredator species
379 increased, aligning with the concept of mesopredator release as proposed by Prugh et al.
380 (2009).

381 The decline of basal tetrapods can be attributed to a combination of direct and indirect drivers.
382 Human activities, including hunting, transportation or agricultural practices, account for a
383 significant portion of tetrapod prey mortality (Hill et al., 2019). Moreover, the mesopredator
384 release phenomenon, amplified by top predators decline (Prugh et al., 2009), may increase
385 predation pressure on basal tetrapods, considering that predation is the primary cause of their
386 mortality (Hill et al., 2019).

387 Beyond these general trends of food-web architecture response to land management intensity,
388 we observed a variety of more specific responses depending on the bioclimatic regions and land
389 uses. For instance, we observed a decrease of omnivory and an increase of trophic chain
390 lengths in response to higher land management intensity in cities and peri-urban areas, partly
391 explaining the unexpected general trends for these two facets. These results support trophic
392 dynamics phenomena previously documented in urbanised habitats called prey specialisation
393 and predator subsidy consumption (Fischer et al., 2012): Dense urban habitats may select
394 mesopredator species specialising on prey adapted to such habitat (prey specialisation), such
395 as certain small bird and rodent species, or mesopredators consuming anthropogenic food
396 (predator subsidy consumption) such as garbage.

397 Context dependencies and discrepant results could also be explained by other forms of human
398 impacts that do not always act in concert with intense land management. For instance, higher
399 habitat fragmentation and diversity were significantly associated with higher intensity only in
400 Mediterranean and Alpine forests (**Figure s9.14**). This may partly explain the singular response
401 of Mediterranean forests, i.e. the decreased connectance and increased compartmentalization.
402 A higher agglomeration of diverse land uses at a small spatial scale is thought to host more
403 diverse independent trophic chains even though empirical evidence is still rare (Gonzalez et al.,
404 2011, Kortsch et al., 2015). Braga et al. (2019) showed, in the same area, that the increase of
405 human footprint was related to a higher compartmentalization, in contradiction with our results.

406 This discrepancy might be due to the difference between land management intensity and
407 human footprint (which incorporate different factors such as night light intensity, road and
408 population density), but also to differences in the analysis methods, such as our choice to
409 control for the context and to use food-web metrics normalised for species richness. When not
410 accounted for, food-web size variability drives important variations in most metrics (Botella et
411 al., 2022), which are not interesting in our context because the effects of human pressures on
412 species richness have been well studied.

413 We acknowledge several limitations in our study stemming from constraints related to the data,
414 spatial resolution, and food-web representation. We used a space-for-time substitution strategy
415 (Walker et al., 2010, Blois et al., 2013) to examine the effects associated with varying land
416 management intensity across space. These spatial effects likely reflect historical changes in
417 intensification occurring over several decades. However, spatial patterns may not always
418 accurately mirror the effects of land use intensification or other global changes (Gaüzère &
419 Devictor, 2021). While we compared areas with similar large-scale bioclimates and land uses,
420 we recognize that small-scale environmental variations covarying with land management
421 intensity, such as elevational gradients in mountain regions, could also impact food-webs
422 architecture and bias our results. Another limitation of our study pertains to the spatial scale
423 used to reconstruct the local meta food-webs (1km²). Some species may have much larger
424 home ranges (e.g. wolf, bear), and interact with other species in neighbouring cells, the extent
425 of which depends not only on the species itself but also on landscape structure. Our cell
426 selection process favoured areas with intense and multi-year sampling efforts, which facilitated
427 the detection of highly mobile species in each occupied cell. Nevertheless, it is possible that we
428 underestimated the presence of the largest and most mobile species, potentially introducing a
429 negative bias in our estimates of apex proportions.

430 Moreover, our study did not account for the dynamic nature of species distributions, primarily
431 relying on species observations over the past 30 years. Consequently, we may have overlooked
432 local declines of species during this period. Improving control for spatial sampling biases could
433 also be achieved through statistical modelling of species detection and absence probabilities
434 (Guillera-Arroita, 2017). Yet, even though such modelling was successfully used with presence-
435 only data from crowdsourcing (van Strien et al., 2013), a better understanding of opportunistic
436 sampling behaviours would be necessary to implement it effectively in our context.

437 Unlike sampled interaction networks, our local meta food-webs are neither snapshots frozen in
438 time, nor limited by the imperfect detection of interactions. Instead, they represent a “maximum”
439 depiction of all the interactions that likely occurred locally over several years, which makes
440 sense in the context of our study (Thuiller et al., 2023). However, these potential trophic
441 interactions may not necessarily manifest locally due to factors like phenological mismatches or
442 low abundances of one or both interacting partners. As a result, we may unintentionally over-
443 emphasize certain rare trophic interactions. Further, local meta food-webs ignore how the
444 realisation of interactions depends on the environment, which might bias our results. To
445 enhance our approach, it would be valuable to conduct a critical comparison with sampled food-
446 webs. Another broader perspective is to integrate non-trophic interactions (Kéfi et al., 2016),
447 interaction strengths (Saint-Béat et al., 2015) and feeding behaviours (Heckmann et al., 2012)
448 into future attempts to characterise interaction network architecture changes.

449 Despite these limitations, our observations fuel the pressing question of the extent of future
450 basal tetrapod collapse due to global changes. Further decline of basal tetrapods could incur
451 further losses of crucial ecosystem services already threatened by climate change, as for
452 instance the control of mosquito borne diseases (Brugueras et al., 2020), and of crop pests
453 (Civantos et al., 2012).

454 **Conclusion.** Land use intensification has already changed the architecture of food-webs, likely
455 affecting ecosystem functions, services, stability and resilience. The general influence of
456 intensification on European tetrapod food-webs consistently undermine top predators. It often
457 decreased the proportion of basal tetrapod species, compartmentalization, and increased
458 connectance and trophic chain lengths. However, some contexts showed marked discrepant
459 responses, such as an increase of basal tetrapod proportions and compartmentalization in
460 Mediterranean forest and Atlantic croplands. Intensive urbanisation especially favoured longer
461 trophic chains and lower omnivory. In summary, intensification has the potential to disrupt the
462 regulation of mesopredators and heighten predation pressure on the basal layer of food webs.
463 This underscores the importance of protecting top predators and raises questions about the
464 long-term stability of food webs in the face of human-induced pressures.

465 **Acknowledgments:**

466 We dedicate this work to the memory of Marc Ohlmann, whose pioneering ideas felt like strong
467 footholds for this modest ascent on the long climbing route towards a biogeography of
468 ecological interaction networks. CB thanks Catherine Matias, Vincent Miele, Stéphane Dray,
469 David M Richardson and Cang Hui for enabling the finalisation of this study.

470

471

472

473

474

475

476

477

478 **References:**

- 479 Agostini, M. G., Roesler, I., Bonetto, C., Ronco, A. E., & Bilenca, D. (2020). Pesticides in the
480 real world: The consequences of GMO-based intensive agriculture on native amphibians.
481 *Biological Conservation*, 241, 108355.
- 482 Ballouard, J. M., Kauffman, C., Besnard, A., Ausanneau, M., Amiguet, M., Billy, G. et al. (2021).
483 Recent invaders in small Mediterranean islands: Wild boars impact snakes in Port-Cros National
484 Park. *Diversity*, 13(10), 498.
- 485 Barabási, A. L., Dezsó, Z., Ravasz, E., Yook, S. H., & Oltvai, Z. (2003, April). Scale-free and
486 hierarchical structures in complex networks. In *AIP Conference Proceedings* (Vol. 661, No. 1,
487 pp. 1-16). American Institute of Physics.
- 488 Blois, J. L., Williams, J. W., Fitzpatrick, M. C., Jackson, S. T., & Ferrier, S. (2013). Space can
489 substitute for time in predicting climate-change effects on biodiversity. *Proceedings of the*
490 *National Academy of Sciences*, 110(23), 9374-9379.
- 491 Botella, C., Dray, S., Matias, C., Miele, V., & Thuiller, W. (2022). An appraisal of graph
492 embeddings for comparing trophic network architectures. *Methods in Ecology and Evolution*,
493 13(1), 203-216. [doi:10.1111/2041-210X.13738](https://doi.org/10.1111/2041-210X.13738)
- 494 Braga, J., Pollock, L. J., Barros, C., Galiana, N., Montoya, J. M., Gravel, D., ... & Thuiller, W.
495 (2019). Spatial analyses of multi-trophic terrestrial vertebrate assemblages in Europe. *Global*
496 *Ecology and Biogeography*, 28(11), 1636-1648.
- 497 Brugueras, S., Fernández-Martínez, B., Martínez-de la Puente, J., Figuerola, J., Porro, T. M.,
498 Rius, C. et al. (2020). Environmental drivers, climate change and emergent diseases
499 transmitted by mosquitoes and their vectors in southern Europe: A systematic review.
500 *Environmental research*, 191, 110038.
- 501 Burchett, W. W., Ellis, A. R., Harrar, S. W., & Bathke, A. C. (2017). Nonparametric inference for
502 multivariate data: the R package nrmv. *Journal of Statistical Software*, 76(1), 1-18.
- 503 Carpio, A. J., Guerrero-Casado, J., Ruiz-Aizpurua, L., Vicente, J., & Tortosa, F. S. (2014). The
504 high abundance of wild ungulates in a Mediterranean region: is this compatible with the
505 European rabbit?. *Wildlife Biology*, 20(3), 161-166.
- 506 Civantos, E., Thuiller, W., Maiorano, L., Guisan, A., & Araújo, M. B. (2012). Potential impacts of
507 climate change on ecosystem services in Europe: the case of pest control by vertebrates.
508 *BioScience*, 62(7), 658-666.
- 509 Clauset, A., Moore, C., & Newman, M. E. (2008). Hierarchical structure and the prediction of
510 missing links in networks. *Nature*, 453(7191), 98-101.
- 511 Clavel, J., Julliard, R., & Devictor, V. (2011). Worldwide decline of specialist species: toward a
512 global functional homogenization?. *Frontiers in Ecology and the Environment*, 9(4), 222-228.
- 513 Corlett, R. T. (2017). Frugivory and seed dispersal by vertebrates in tropical and subtropical
514 Asia: an update. *Global Ecology and Conservation*, 11, 1-22.

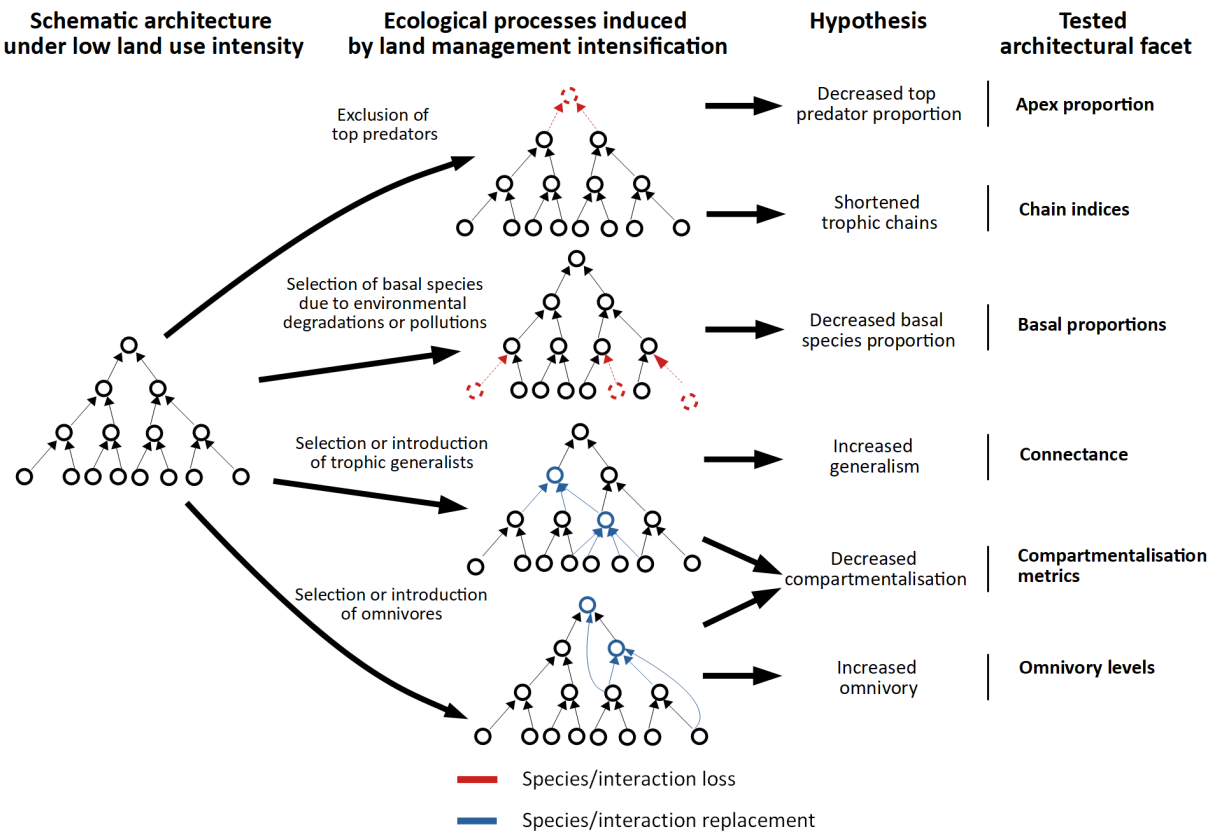
- 515 Diaz, S., Settele, J., Brondizio, E., et al (2019). Summary for policymakers of the global
516 assessment report on biodiversity and ecosystem services.
- 517 Dobson, A., Lodge, D., Alder, J., Cumming, G. S., Keymer, J., McGlade, J. et al. (2006). Habitat
518 loss, trophic collapse, and the decline of ecosystem services. *Ecology*, 87(8), 1915-1924.
519 Doherty, T. S., Glen, A. S., Nimmo, D. G., Ritchie, E. G., & Dickman, C. R. (2016). Invasive
520 predators and global biodiversity loss. *Proceedings of the National Academy of Sciences*,
521 113(40), 11261-11265.
- 522 De Visser, S. N., Freymann, B. P., & Olf, H. (2011). The Serengeti food web: empirical
523 quantification and analysis of topological changes under increasing human impact. *Journal of*
524 *animal ecology*, 80(2), 484-494.
- 525 De Vries, F. T., Thébault, E., Liiri, M., Birkhofer, K., Tsiafouli, M. A., Bjørnlund, L., ... & Bardgett,
526 R. D. (2013). Soil food web properties explain ecosystem services across European land use
527 systems. *Proceedings of the National Academy of Sciences*, 110(35), 14296-14301.
528
- 529 Dou, Y., Cosentino, F., Malek, Z. *et al.* A new European land systems representation accounting
530 for landscape characteristics. *Landscape Ecology* 36, 2215–2234 (2021).
531 <https://doi.org/10.1007/s10980-021-01227-5>
532
- 533 European Environmental Agency, EEA (2021). Biogeographical regions.
534 <https://www.eea.europa.eu/data-and-maps/data/biogeographical-regions-europe-3>
535
- 536 Estes, J. A., Terborgh, J., Brashares, J. S., Power, M. E., Berger, J., Bond, W. J. et al. (2011).
537 Trophic downgrading of planet Earth. *science*, 333(6040), 301-306.
538
- 539 Etard, A., Pigot, A.L. & Newbold, T. (2022). Intensive human land uses negatively affect
540 vertebrate functional diversity. *Ecology Letters* 25: 330-343. DOI:10.1111/ele.13926.
541
- 542 Evans, D. M., Pocock, M. J., & Memmott, J. (2013). The robustness of a network of ecological
543 networks to habitat loss. *Ecology letters*, 16(7), 844-852.
- 544 Fahrig, L. (2003). Effects of habitat fragmentation on biodiversity. *Annual review of ecology,*
545 *evolution, and systematics*, 34(1), 487-515.
- 546 Fischer, J. D., Cleeton, S. H., Lyons, T. P., & Miller, J. R. (2012). Urbanization and the predation
547 paradox: the role of trophic dynamics in structuring vertebrate communities. *Bioscience*, 62(9),
548 809-818.
- 549 Gaüzère, P., & Devictor, V. (2021). Mismatches between birds' spatial and temporal dynamics
550 reflect their delayed response to global changes. *Oikos*, 130(8), 1284-1296.
- 551 Gaüzère, P., O'Connor, L., Botella, C., Poggiato, G., Münkemüller, T., Pollock, L. J., ... &
552 Thuiller, W. (2022). The diversity of biotic interactions complements functional and phylogenetic
553 facets of biodiversity. *Current Biology*, 32(9), 2093-2100.
- 554 Geiger, F., Bengtsson, J., Berendse, F., Weisser, W. W., Emmerson, M., Morales, M. B. et al
555 (2010). Persistent negative effects of pesticides on biodiversity and biological control potential
556 on European farmland. *Basic and Applied Ecology*, 11(2), 97-105.

- 557 Gonzalez, A., Rayfield, B., & Lindo, Z. (2011). The disentangled bank: how loss of habitat
558 fragments and disassembles ecological networks. *American journal of botany*, 98(3), 503-516.
- 559 Gilarranz, L. J., Mora, C., & Bascompte, J. (2016). Anthropogenic effects are associated with a
560 lower persistence of marine food webs. *Nature communications*, 7(1), 1-5.
- 561 Gossner, M. M., Lewinsohn, T. M., Kahl, T., Grassein, F., Boch, S., Prati, D. et al. (2016). Land-
562 use intensification causes multitrophic homogenization of grassland communities. *Nature*,
563 540(7632), 266-269.
- 564 Guillera-Arroita, G. (2017). Modelling of species distributions, range dynamics and communities
565 under imperfect detection: advances, challenges and opportunities. *Ecography*, 40(2), 281-295.
- 566 Hallmann, C. A., Foppen, R. P., Van Turnhout, C. A., De Kroon, H., & Jongejans, E. (2014).
567 Declines in insectivorous birds are associated with high neonicotinoid concentrations. *Nature*,
568 511(7509), 341-343.
- 569 Heckmann, L., Drossel, B., Brose, U., & Guill, C. (2012). Interactive effects of body-size
570 structure and adaptive foraging on food-web stability. *Ecology letters*, 15(3), 243-250.
- 571
572 Heger, T., & Jeschke, J. M. (2018). Enemy release hypothesis. *Invasion Biology. Hypotheses
573 and Evidence*. 1st ed. Boston, MA: CABI, 92-102.
- 574
575 Herbst, C., Wäschke, N., Barto, E. K., Arnold, S., Geuß, D., Halboth, I. et al. (2013). Land use
576 intensification in grasslands: higher trophic levels are more negatively affected than lower
577 trophic levels. *Entomologia Experimentalis et Applicata*, 147(3), 269-281.
- 578
579 Hill, J. E., DeVault, T. L., & Belant, J. L. (2019). Cause-specific mortality of the world's terrestrial
580 vertebrates. *Global Ecology and Biogeography*, 28(5), 680-689.
- 581
582 IUCN (International Union for Conservation of Nature) 2021. The IUCN Red List of Threatened
583 Species. Version 2021-1. <https://www.iucnredlist.org>. Downloaded on 15 march 2021.
- 584
585 Johnson, R. A., and D. W. Wichern. 1992. Applied multivariate statistical analysis. Third edition.
586 Prentice–Hall, Englewood Cliffs, New Jersey, USA.
- 587
588 Kéfi, S., Miele, V., Wieters, E. A., Navarrete, S. A., & Berlow, E. L. (2016). How structured is the
589 entangled bank? The surprisingly simple organization of multiplex ecological networks leads to
590 increased persistence and resilience. *PLoS biology*, 14(8), e1002527.
- 591
592 Keyes, A. A., McLaughlin, J. P., Barner, A. K., & Dee, L. E. (2021). An ecological network
593 approach to predict ecosystem service vulnerability to species losses. *Nature communications*,
594 12(1), 1-11.
- 595
596 Kortsch, S., Primicerio, R., Fossheim, M., Dolgov, A. V., & Aschan, M. (2015). Climate change
597 alters the structure of arctic marine food webs due to poleward shifts of boreal generalists.
598 *Proceedings of the Royal Society B: Biological Sciences*, 282(1814), 20151546.
- 599
600 Kortsch, S., Primicerio, R., Aschan, M., Lind, S., Dolgov, A. V., & Planque, B. (2019). Food-web
601 structure varies along environmental gradients in a high-latitude marine ecosystem. *Ecography*,
602 42(2), 295-308.
- 603

- 604
605 Lange, H. J. D., Lahr, J., Van der Pol, J. J., Wessels, Y., & Faber, J. H. (2009). Ecological
606 vulnerability in wildlife: an expert judgment and multicriteria analysis tool using ecological traits
607 to assess relative impact of pollutants. *Environmental Toxicology and Chemistry: An*
608 *International Journal*, 28(10), 2233-2240.
- 609
610 Li, D., Poisot, T., Waller, D. M., & Baiser, B. (2018). Homogenization of species composition
611 and species association networks are decoupled. *Global Ecology and Biogeography*, 27(12),
612 1481-1491.
- 613
614 Link, J. S., Stockhausen, W. T., & Methratta, E. T. (2005). Food-web theory in marine
615 ecosystems. *Aquatic food webs: an ecosystem approach*. Oxford University Press, Oxford, 98-
616 114.
- 617
618 Liu, C., Bathke, A. C., & Harrar, S. W. (2011). A nonparametric version of Wilks' lambda—
619 Asymptotic results and small sample approximations. *Statistics & probability letters*, 81(10),
620 1502-1506.
- 621
622 MacKay, R. S., Johnson, S., & Sansom, B. (2020). How directed is a directed network?. *Royal*
Society open science, 7(9), 201138.
- 623
624 Maiorano, L., Montemaggiore, A., Ficetola, G. F., O'connor, L., & Thuiller, W. (2020). TETRA-EU
625 1.0: A species-level trophic metaweb of European tetrapods. *Global Ecology and Biogeography*,
29(9), 1452-1457.
- 626
627 McKinney, M. L., & Lockwood, J. L. (1999). Biotic homogenization: a few winners replacing
many losers in the next mass extinction. *Trends in ecology & evolution*, 14(11), 450-453.
- 628
629 Mestre, F., Rozenfeld, A., & Araújo, M. B. (2022). Human disturbances affect the topology of
food webs. *Ecology Letters*.
- 630
631 Montoya, J. M., Rodríguez, M. A., & Hawkins, B. A. (2003). Food web complexity and higher-
level ecosystem services. *Ecology letters*, 6(7), 587-593.
- 632
633 Newman, M. E. (2006). Modularity and community structure in networks. *Proceedings of the*
national academy of sciences, 103(23), 8577-8582.
- 634
635 O'Connor, L. M., Pollock, L. J., Braga, J., Ficetola, G. F., Maiorano, L., Martinez-Almoyna, C. et
636 al. (2020). Unveiling the food webs of tetrapods across Europe through the prism of the Eltonian
niche. *Journal of Biogeography*, 47(1), 181-192.
- 637
638 Poisot, T., Canard, E., Mouillot, D., Mouquet, N., & Gravel, D. (2012). The dissimilarity of
species interaction networks. *Ecology letters*, 15(12), 1353-1361.
- 639
640 Prugh, L. R., Stoner, C. J., Epps, C. W., Bean, W. T., Ripple, W. J., Laliberte, A. S., &
Brashares, J. S. (2009). The rise of the mesopredator. *Bioscience*, 59(9), 779-791.
- 641
642 Rigal, S., Devictor, V., Gaüzère, P., Kéfi, S., Forsman, J. T., Kajanus, M. H. et al. (2021). Biotic
643 homogenisation in bird communities leads to large-scale changes in species associations.
Oikos.

- 644 Saint-Béat, B., Baird, D., Asmus, H., Asmus, R., Bacher, C., Pacella, S. R. et al. (2015). Trophic
645 networks: How do theories link ecosystem structure and functioning to stability properties? A
646 review. *Ecological indicators*, 52, 458-471.
- 647 Sparling, D. W., Fellers, G., & McConnell, L. (2001). Pesticides are involved with population
648 declines of amphibians in the California Sierra Nevadas. *The scientific world journal*, 1, 200-201.
- 649 Thuiller, W., Calderon-Sanou, I., Chalmandrier, L., Gaüzere, P., O'Connor, L., Ohlmann, M.,
650 Poggiato, G. & Münkemüller, T. (2023). Navigating the integration of Biotic Interactions in
651 Biogeography. *Journal of Biogeography*. [In press]
- 652 Tylianakis, J. M., Laliberté, E., Nielsen, A., & Bascompte, J. (2010). Conservation of species
653 interaction networks. *Biological conservation*, 143(10), 2270-2279.
- 654 Van Strien, A. J., Van Swaay, C. A., & Termaat, T. (2013). Opportunistic citizen science data of
655 animal species produce reliable estimates of distribution trends if analysed with occupancy
656 models. *Journal of Applied Ecology*, 50(6), 1450-1458.
- 657 Walker, L. R., Wardle, D. A., Bardgett, R. D., & Clarkson, B. D. (2010). The use of
658 chronosequences in studies of ecological succession and soil development. *Journal of ecology*,
659 98(4), 725-736.
- 660 Wermelinger, B. and Herrmann, M. (2015). Chapter 7 - Natural Enemies of Bark Beetles:
661 Predators, Parasitoids, Pathogens, and Nematodes. (Pages 247-304)
662
663

664 Figures

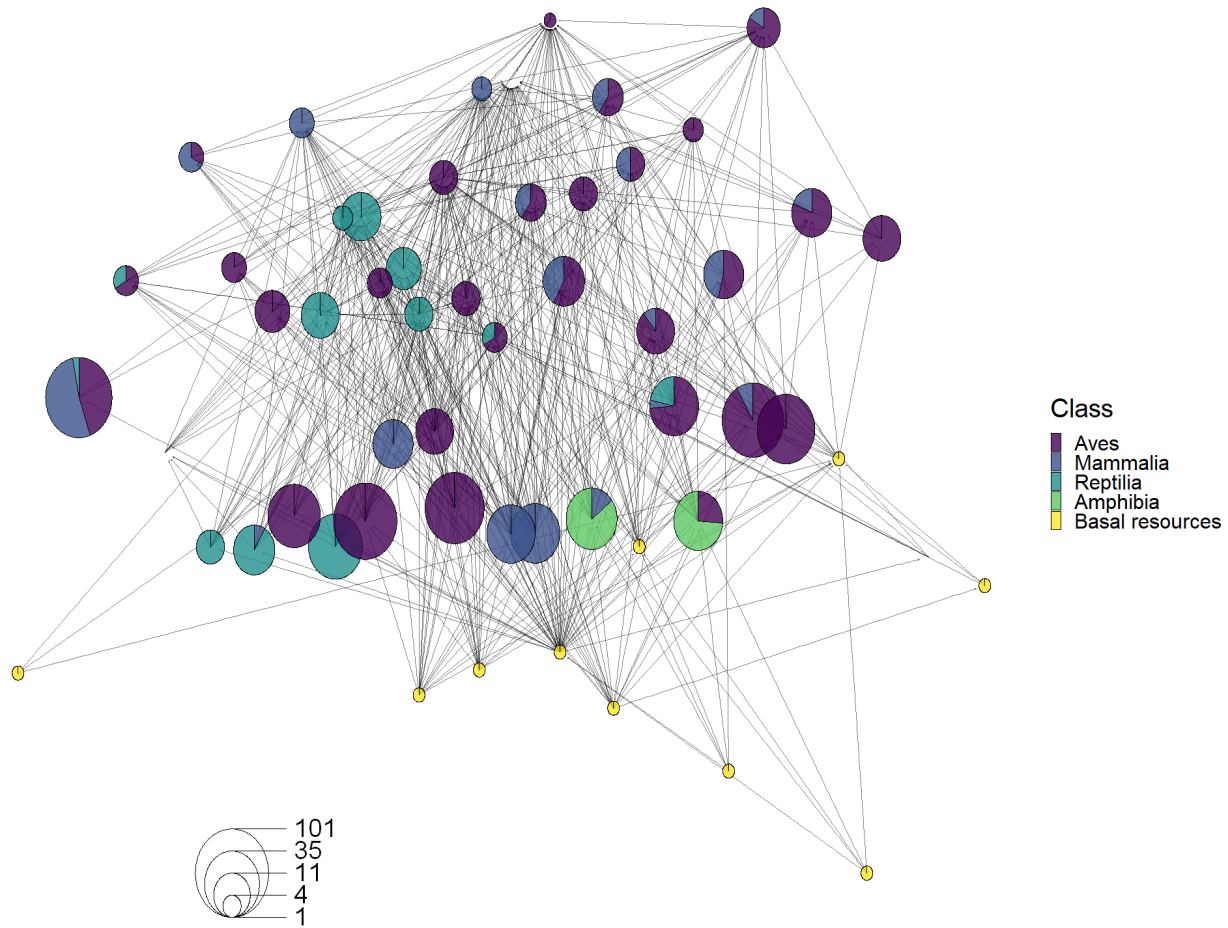


665

666 **Figure 1.** Hypothetical food-web architecture changes related to the ecological processes
 667 associated with land use intensification. However, our general assumptions could be
 668 contradicted by the context dependence of these processes, i.e. intensification does not
 669 necessarily enhance all these processes under all land uses or climates, their interactions and
 670 the effect of other unknown processes.

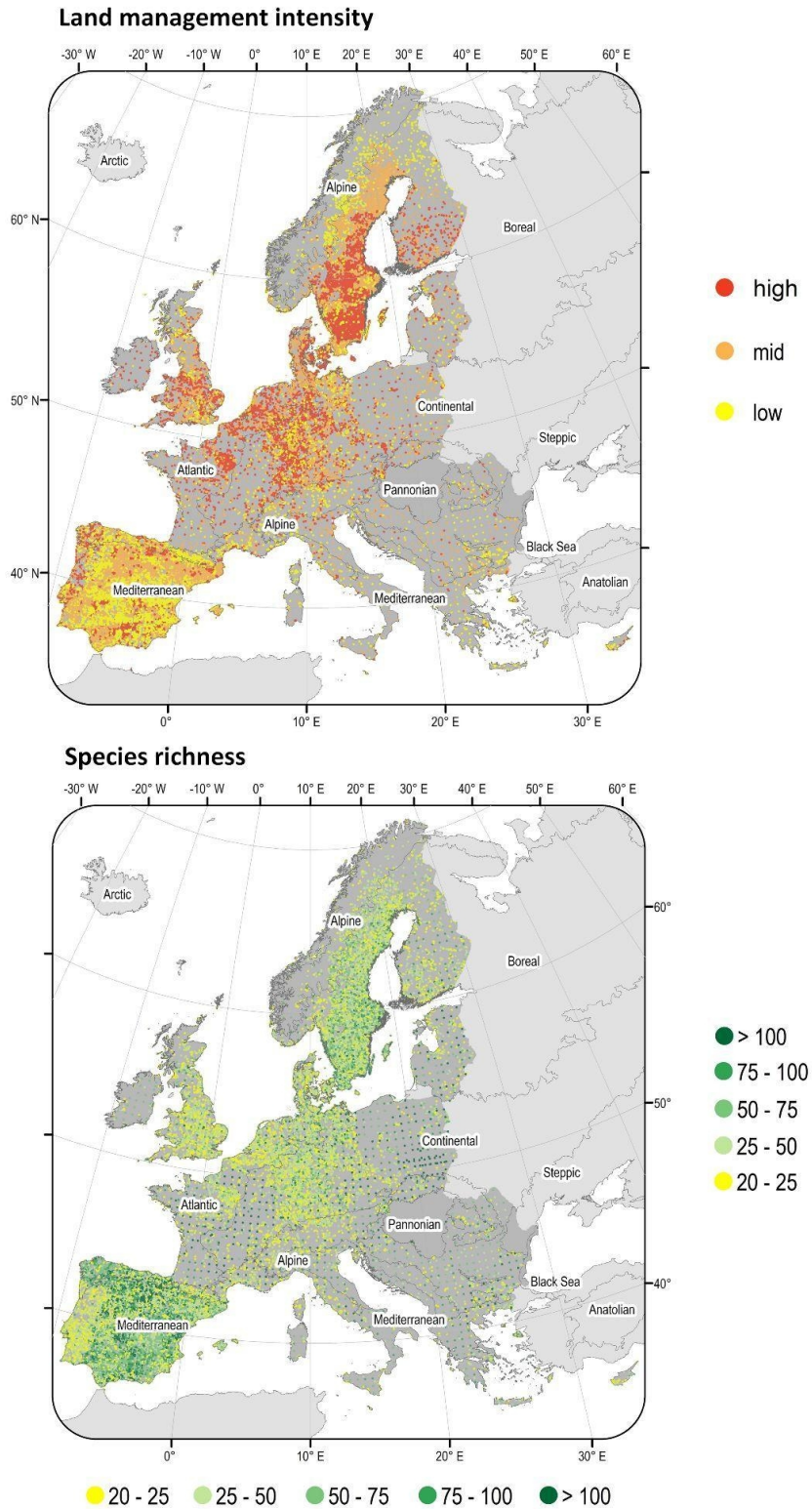
671

672



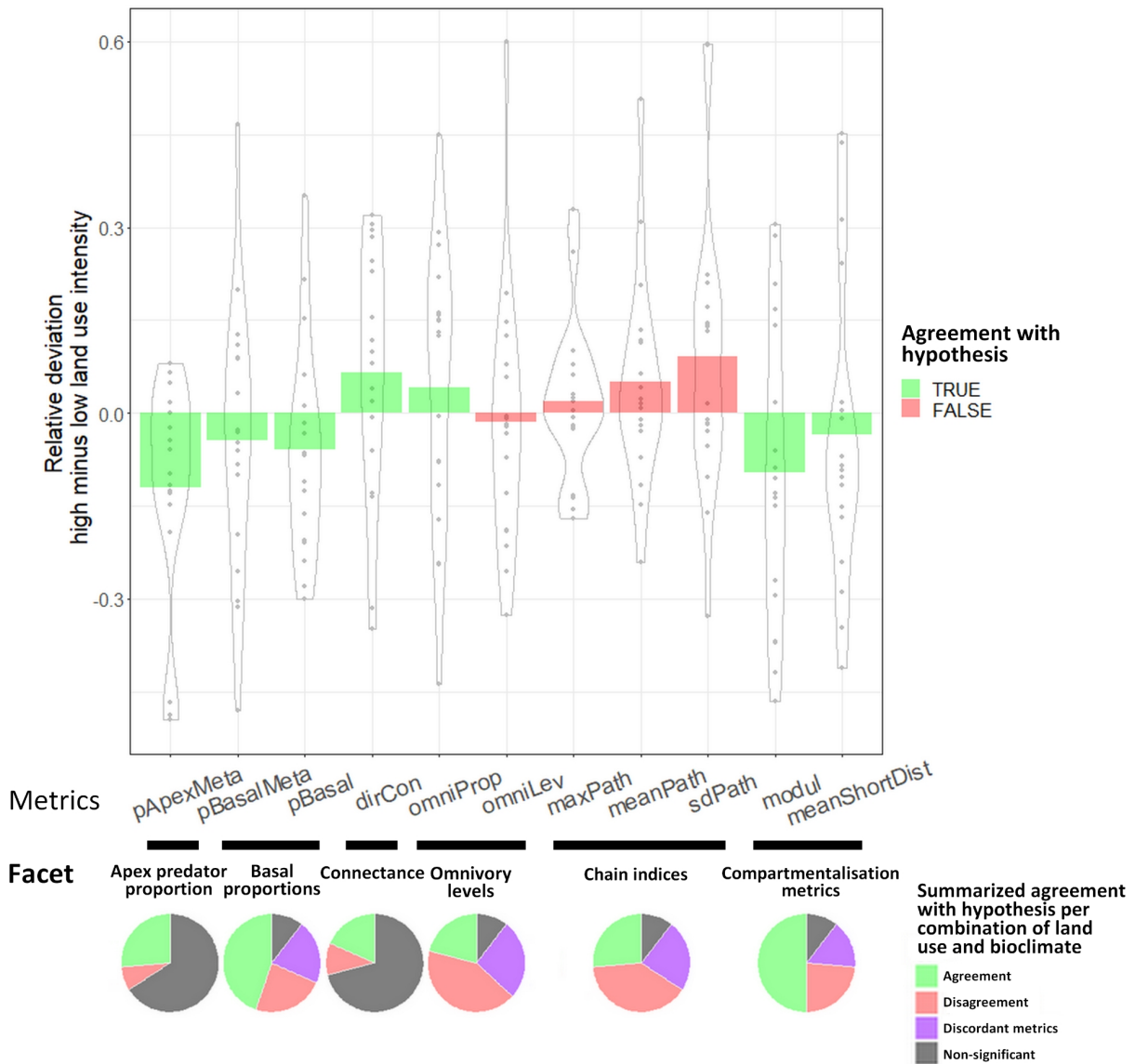
673

674 **Figure 2.** The metaweb of trophic interactions of our 756 European tetrapods aggregated per
 675 trophic groups (O'Connor et al., 2020). Each node is one of the 46 trophic groups (detailed in
 676 Table **S2.1**), its size represents the number of species while the colours represent the
 677 proportion of classes. The trophic groups were automatically positioned vertically according to
 678 their trophic level and horizontally so that connected groups are more aligned than non-
 679 connected ones (TL-tsne layout method of the R package **metanetwork**:
 680 <https://marcohlmann.github.io/metanetwork/>). Basal resources (i.e. diets that are not wild
 681 vertebrates) were included as yellow nodes.

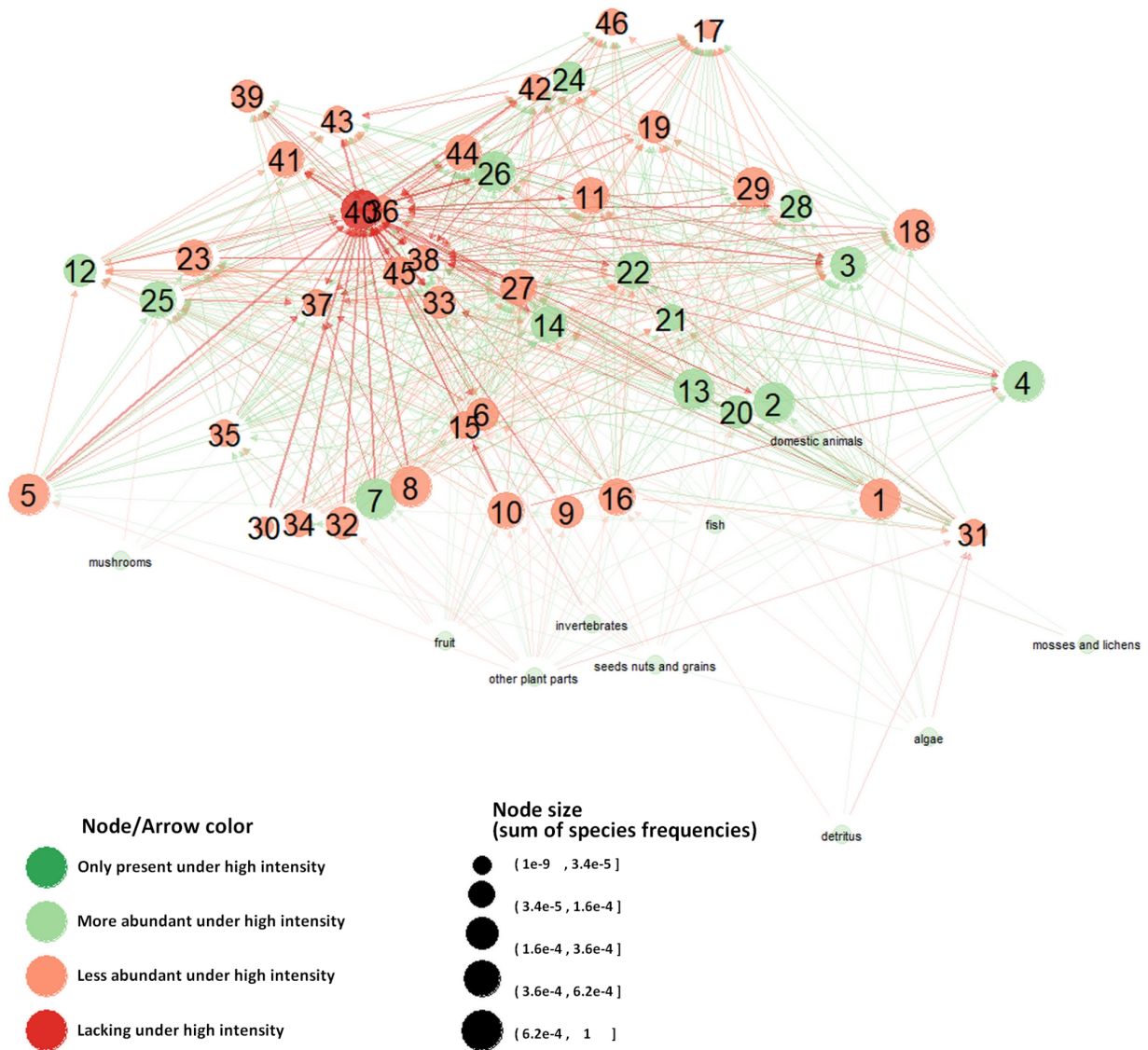


682

683 **Figure 3.** Map of the 67,051 studied local meta food-webs (1km² cells). **Top:** Cell locations
 684 colored by land management intensity. **Bottom:** Cell locations colored by observed species
 685 richness.



688 **Figure 4.** Food-web metric deviations related to higher land management intensity per
 689 architecture facet and agreement with the initial hypothesis. **Top:** For each metric (x-axis), the
 690 relative deviation (barplot on y-axis) is the average over 18 contexts (grey dots) of the mean
 691 deviation from low to high intensity food-webs divided by the interquartile range of the global
 692 metric distribution. This relative deviation indicates the general response to land management
 693 intensity while controlling for context-dependence. The bar plot's colour indicates if the deviation
 694 is confirming (green) or contradicting (red) the initial hypothesis on the corresponding facet (see
 695 **Figure 1**). **Bottom:** For each facet, a pie plot summarises the tests of deviation significance
 696 over the 38 contexts and intensity level comparisons (high versus low and medium versus low)
 697 into agreements (green) or disagreements (red) with the hypothesis, discordant metrics (purple)
 698 or non-significant, based on the multivariate test.



699

700 **Figure 5.** Changes of trophic group frequencies when increasing land management intensity.
 701 This difference plot between average networks in high and low land management intensity cells
 702 is produced by the `diff_plot` function in **metanetwork** R package. As in **Figure S2.2**, each node
 703 is one trophic group and its size represents the sum of species frequencies across the 67,051
 704 local meta food-webs. A red (resp. green) node colour indicates a decrease (resp. increase) of
 705 the group frequency in high intensity cells compared to low intensity cells. More details on the
 706 trophic group compositions are provided in Table **S2.1**.

707

708

709

710

711

712 **Tables**

713

Architecture facet	Metric acronym	Description	Range of values
Apex proportion	pApexMeta	Proportion of species that are apex predators in the metaweb.	[0,0.3]
Basal proportions	pBasalMeta	Proportion of species that are basal in the metaweb.	[0,1]
	pBasal	Proportion of species that are basal in the local meta food-web (have no preys).	[0.1,1]
Connectance	dirCon	Directed connectance: density of interactions in the local meta food-web.	[0,0.3]
Omnivory Levels	omniProp	Proportion of general omnivore species among non-basal and non-top species.	[0.3,1]
	omniLvl	Mean standard deviation of prey trophic levels of the non-basal and non-top species.	[0.1,0.7]
Chain indices	maxPath	Maximum length across shortest-paths from basal to apex species in the local meta food-web.	[0,12]
	meanPath	Mean length across shortest-paths from basal to apex species in the local meta food-web.	[0,3.8]
	sdPath	Standard deviation of lengths across shortest-paths from basal to apex species in the local meta food-web.	[0,2.4]
Compartment alization metrics	modul	Modularity (Newman et al., 2006): A measure of densely interconnected groups of species being less connected with other species.	[-1,0.4]
	meanShortDist	Mean path distance across species pairs in the undirected transform of the local meta food-web.	[1,4.3]

714 **Table 1.** Architectural facets and their constituent metrics computed for all local food-webs in
715 this study.

716

717

718

Appendices

719

720 **Appendix S1 - Data preprocessing**

721

722 **Figure S1.1** summarizes the 4 steps of our data preprocessing pipeline leading to the selection
723 of the species, cells and combinations of bioclimatic region, land use and land management
724 intensity in this study. In the text below, we also present in more detail the first step, namely

725 data cleaning of the GBIF/iNaturalist occurrences. Finally, we explain how to reproduce the data
726 preprocessing steps for transparency (optional) and the manuscript Figures using our online
727 repositories.

728

729 **Data cleaning (step 1 of Figure S1.1).** We extracted all tetrapod geolocated occurrences from
730 the GBIF (except iNaturalist dataset) with date posterior to 1980, including only human
731 observations, a geolocation uncertainty below 1km (resolution of our study cells). Besides, we
732 extracted the tetrapod iNaturalist research grade occurrences using the `rinat` R package to add
733 them to the GBIF ones. Then, we removed duplicates, and occurrences suffering from various
734 coordinates errors using the **CoordinateCleaner** R library:

- 735 - Degree-minute to decimal degree conversion error (`cd_ddmm` function)
- 736 - Location too close to gbif headquarters or other biodiversity institutions, country capitals,
737 country centroids.
- 738 - Occurrences outside of the IUCN range, if available and including the invasive range
739 (spatial ranges are assessed in the context of the IUCN red list of threatened species,
740 IUCN, 2021), for the corresponding species. Indeed, we assumed that species presence
741 outside of the IUCN range was either an identification error, a geolocation error, or a
742 vagrant specimen not proving the existence of a local population.

743 We fully removed the datasets for which the `cd_round` function of **CoordinateCleaner**
744 detected a spatial rasterization pattern in their coordinates with a periodicity superior to 1km.
745 However, we acknowledge that this automatic detection algorithm was not sufficient to detect all
746 rasterized datasets as for instance one of them is visible from Figure 3-bottom. Finally, the 756
747 species included in this study were those with at least one occurrence remaining and present in
748 the tetrapod meta-web of trophic interactions (Maiorano et al., 2020).

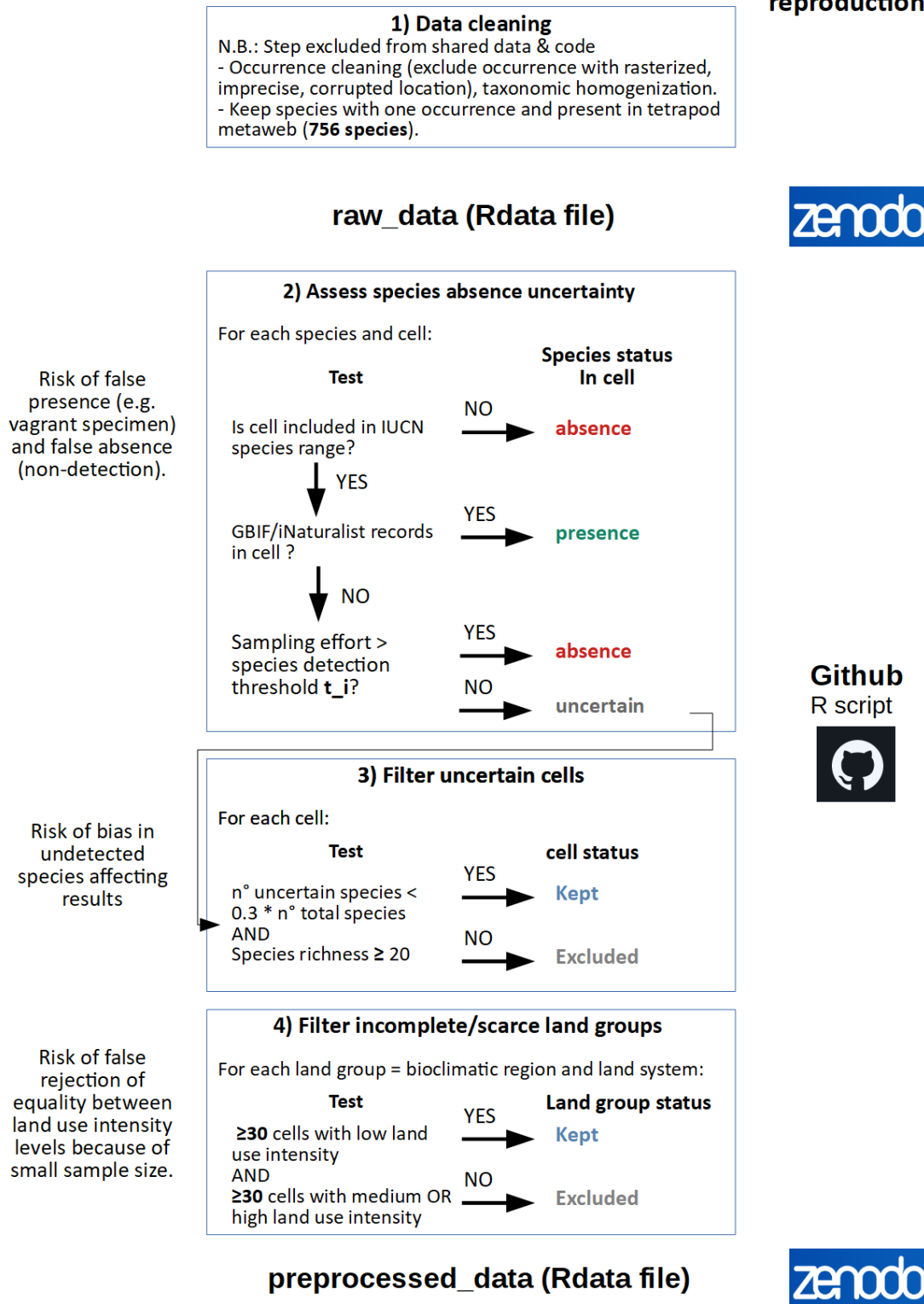
749

750 **Reproduction.** To reproduce our result Figures, one can simply download **preprocessed_data**
751 and **TrophicNetworksList** Rdata files from our Zenodo repository
752 (<https://zenodo.org/record/5831144>) and run R script **analyse_preprocessed_data.R** provided
753 in our Github repository (https://github.com/ChrisBotella/foodwebs_vs_land_use). It will
754 generate the Figures of this manuscript locally. To reproduce steps 2 to 4 of the data
755 preprocessing pipeline given in **Figure S1.1** from the cleaned GBIF/iNaturalist occurrences, it is
756 possible to download the **raw_data** Rdata file from Zenodo (several Gb file) and run the
757 **preprocess_data.R** script from our Github. It will re-generate **preprocessed_data** and
758 **TrophicNetworksList** locally, which are the inputs for **analyse_preprocessed_data.R**.

759

Error control

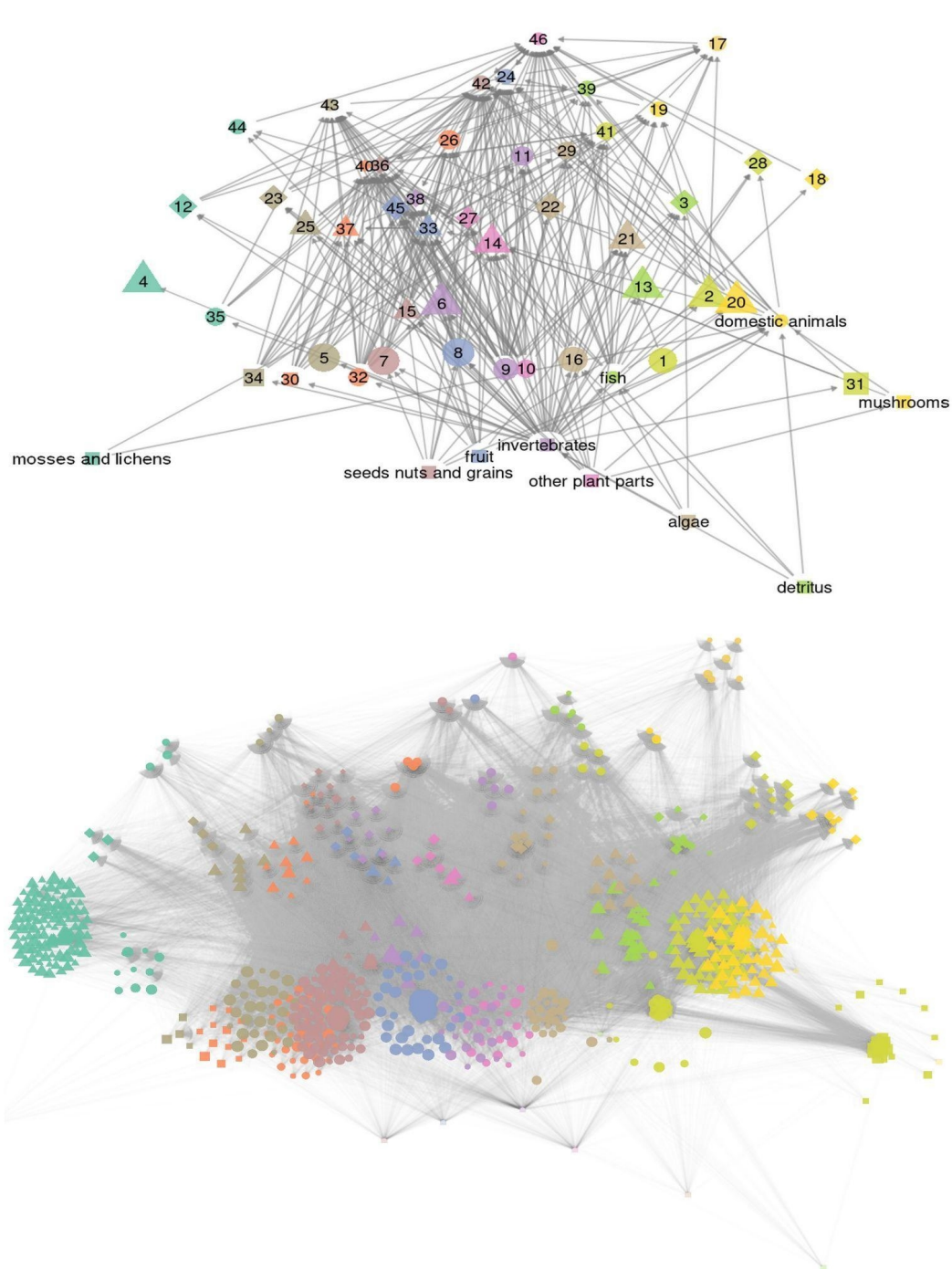
Steps

Access/
reproduction

760

761 **Figure S1.1.** Data preprocessing pipeline (center), potential errors that each step is meant to
762 control (left) and the websites where our material is provided for reproduction (right).

763 **Appendix S2 - metaweb details**



764
 765 **Figure S2.2** The metaweb of trophic interactions of our 756 European tetrapod species and
 766 their 46 trophic groups. Top: The meso-scale metaweb where each node is one trophic group
 767 numbered as in Table S2.1, and identified by a combination of shape and colour. The vertical
 768 positioning is based on the trophic level, while the horizontal one is based on the proximity in
 769 the network (more connected groups are more aligned than non-connected ones). Diets are
 770 included as basal nodes. Each arrow indicates trophic interactions between species of two
 771 groups (going from prey to predator). Bottom: The micro scale metaweb where each node is
 772 one species and species belonging to a same trophic group are aggregated into clusters (group-

773 TL-tsne method of the R package metanetwork) with the same trophic group shape and colour
 774 code as in the above Figure.
 775
 776

Group	nSpecies	Most frequent species	Most common class
46	1	Bubo bubo	Aves
17	6	Accipiter gentilis	Aves
24	1	Strix aluco	Aves
42	2	Vulpes vulpes	Mammalia
39	5	Aquila chrysaetos	Aves
43	3	Felis silvestris	Mammalia
19	2	Falco peregrinus	Aves
44	3	Circaetus gallicus	Mammalia
41	4	Ciconia ciconia	Aves, Mammalia
26	4	Corvus corone	Aves
29	4	Milvus milvus	Aves
11	5	Buteo buteo	Aves
28	11	Circus aeruginosus	Aves
36	11	Malpolon monspessulanus	Reptilia
40	2	Dolichophis caspius	Reptilia
18	9	Hieraaetus pennatus	Aves
23	3	Athene noctua	Aves
38	7	Vipera berus	Reptilia
3	11	Larus canus	Aves
12	3	Accipiter nisus	Aves
22	12	Chroicocephalus ridibundus	Aves
45	3	Lanius excubitor	Aves
27	4	Lanius collurio	Aves
25	7	Nucifraga caryocatactes	Aves
33	4	Timon lepidus	Reptilia
37	9	Coronella girondica	Reptilia
21	9	Ardea cinerea	Aves
14	3	Garrulus glandarius	Aves
4	101	Cuculus canorus	Mammalia
13	23	Vanellus vanellus	Aves
2	67	Columba palumbus	Aves
20	48	Gallinago gallinago	Aves
6	9	Turdus merula	Aves
15	11	Eliomys quercinus	Mammalia
35	11	Anguis fragilis	Reptilia
8	54	Fringilla coelebs	Aves
5	31	Hirundo rustica	Aves
16	27	Bufo bufo	Amphibia
1	23	Gyps fulvus	Amphibia
7	77	Parus major	Aves
10	24	Crocidura russula	Mammalia
9	22	Apodemus sylvaticus	Mammalia
32	35	Zootoca vivipara	Reptilia
34	4	Chalcides striatus	Reptilia
30	12	Chalcides bedriagai	Reptilia
31	29	Lissotriton vulgaris	Amphibia

777
 778 **Table S2.1.** The 46 trophic groups of the European tetrapod metaweb as defined in O'Connor et
 779 al. (2020) and represented in Figure S2.2-bottom above and Figure 4 of the main manuscript.

780 Groups are ordered by decreasing average trophic level. The table also shows their number of
 781 species (of the 756 studied here), the most frequently present species across the 67,051 local
 782 meta food-webs and the most common taxonomic class of the group.

783

784 **Appendix S3- Land systems and study area coverage**

785

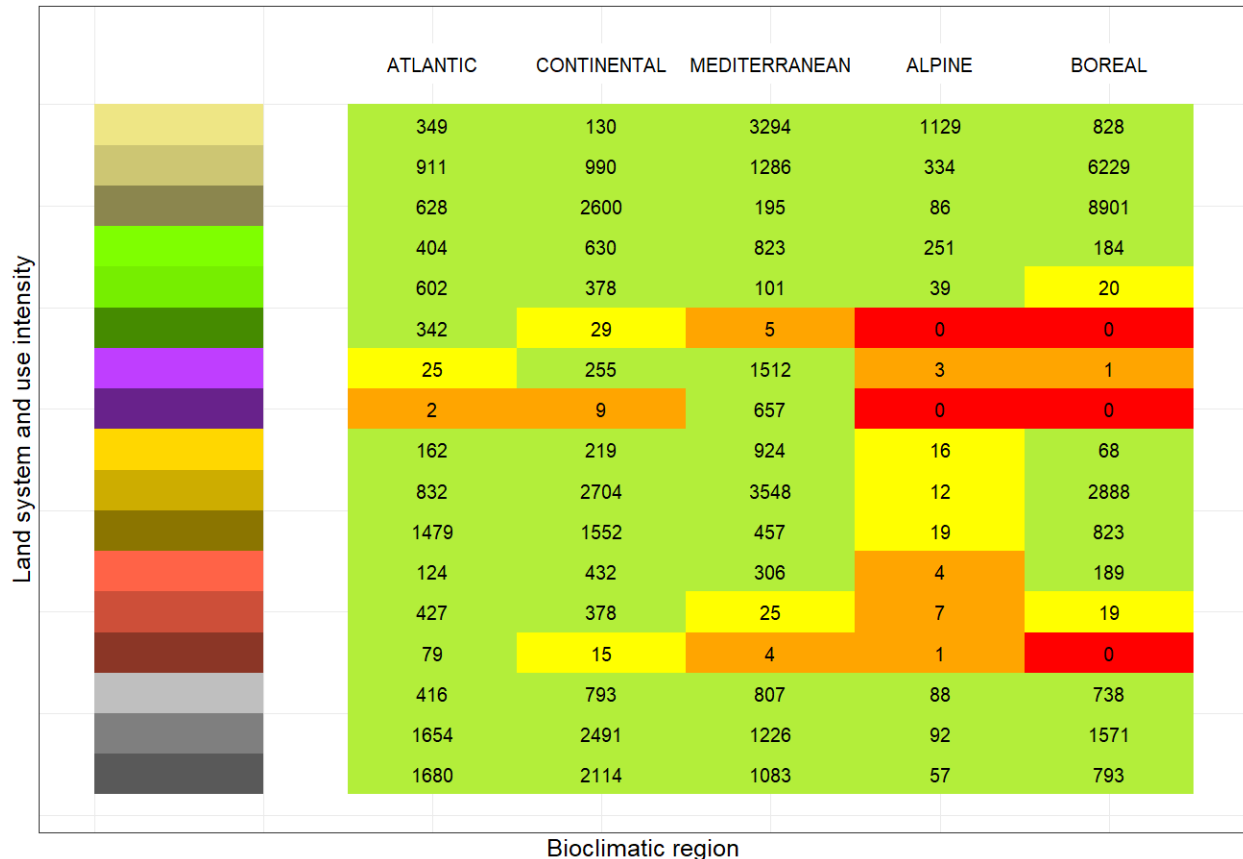
786

land uses	Composition	Land management intensity classes	Indicators of intensity used
1. Forest	All forests except some clear cuts	Low, medium, high	Wood production, probability of primary forest
2. Grassland	All grasslands excluding grassed wetlands	Low, medium, high	Inorganic fertilizer input, mowing frequency, livestock density
3. Permanent cropland	vineyards, olive groves, fruit gardens	Extensive (low), Intensive (high)	Understory vegetation
4. Arable cropland	Annual crops (wheat, etc)	Low, medium, high	Inorganic fertilizer input, field size
5. Agricultural mosaic	cropland and grassland	Low, medium, high	Inorganic fertilizer input, field size, livestock density
6. Human settlement	Cities and surrounding urban areas	Low, medium, high	Population density, distance from urban core, imperviousness

787

Table S3.2. Classification of land uses and land management intensity.

788



789

790

791

792

793

794

795

796

797

798

799

800

801

802

803

804

805

806

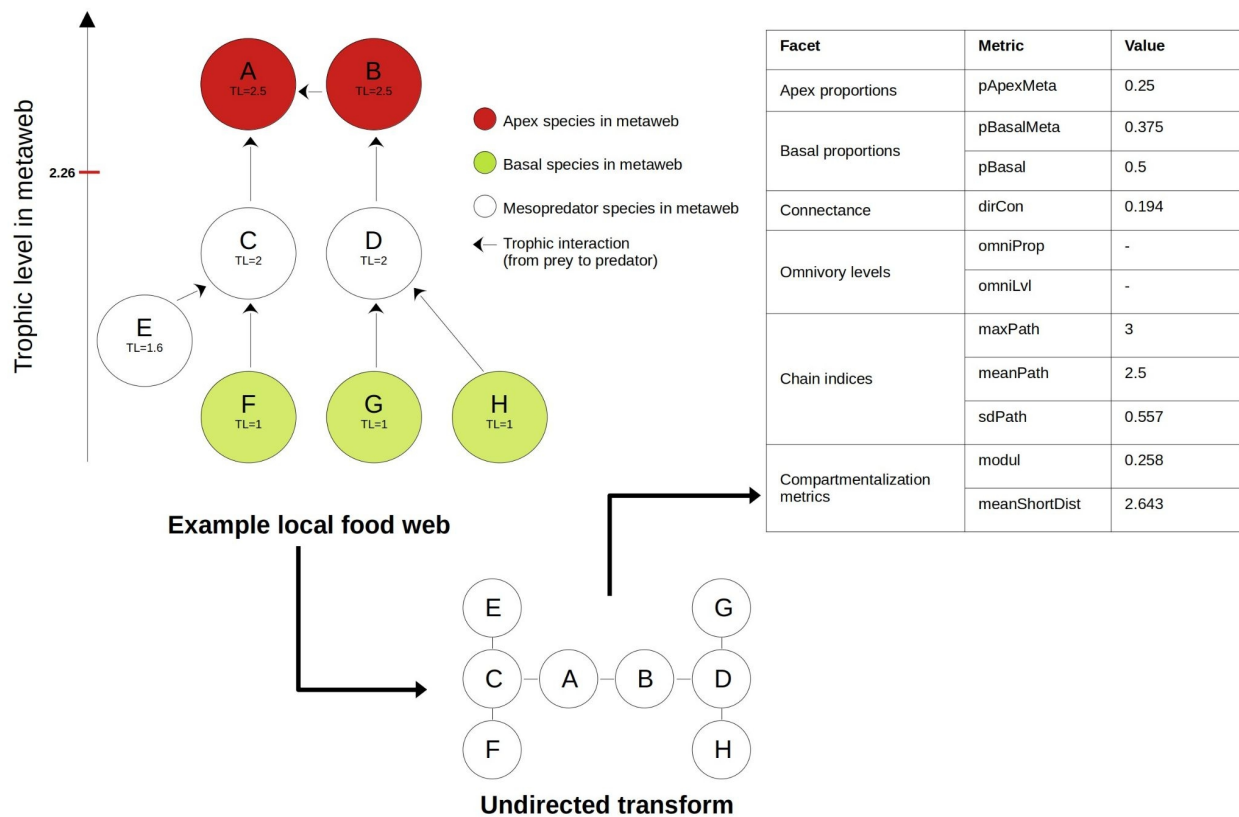
Appendix S4- Detailed network metrics per architecture facet

807

808

Apex proportion: To define apex species, we first computed species trophic levels (MacKay et al., 2020) in the metaweb completed with species diets (Figure S2.2), as recommended by

809 Maiorano et al. (2020). There are 10 diets (1) “algae”, (2) “fish”, (3) “invertebrates”, (4) “domestic
 810 animals”, (5) “mushrooms”, (6) “mosses and lichens”, (7) “detritus”, (8) “fruit”, (9) “seed, nuts
 811 and grains” and (10) “other plant parts”. They were integrated as additional nodes in the
 812 metaweb along with trophic relationships between them, that is: (1), (7) is eaten by (2) and (3).
 813 (3) is eaten by (2) and (4). (5), (6), (7), (8), (9), (10) are eaten by (4). (10) is eaten by (5). This
 814 makes the trophic levels more meaningful, especially for the many tetrapod species that
 815 otherwise have no prey among tetrapods, because they can have variable height in the whole
 816 trophic chains including non-tetrapod species. We define that species with trophic level above
 817 2.262 are apex predators, so that the 59 selected species fitted best to those generally qualified
 818 as apex predators, including wolf, brown bear, wolverine, foxes, badger, wild cat, eagles,
 819 falcons, owls, and macro vipers. We then computed, in each local network, the proportion of
 820 apex predators, hereafter called **pApexMeta**. In the example local meta food-web of **Figure**
 821 **S4.5**, there are two species that are apex in the metaweb (their trophic level is higher than 2.26)
 822 so $pApexMeta=2/8=0.25$.



823

824 **Figure S4.5.** Virtual example of a local food-web and the values of our metrics. Eight species
 825 are present in this virtual trophic community, and they are positioned vertically according to their

826 trophic level in the metaweb of tetrapod species. If a species has no tetrapod prey in the
827 metaweb, it is a basal species (filled in green), if its trophic level is above 2.26, it is an apex
828 predator (filled in red), otherwise it is a mesopredator. The compartmentalization metrics are
829 computed from the undirected transform of the food-web, which is represented in the bottom.

830 Basal proportions: We computed the proportion of basal species in the local network (species
831 with no prey), called **pBasal**, and the proportion of species that are basal in the metaweb
832 (species without any tetrapod prey in the metaweb), called **pBasalMeta**. This gives a different
833 perspective as a non-basal species in the metaweb can be locally observed without its prey. In
834 the example local food-web of **Figure S4.5**, there are three species that are basal in the
835 metaweb (F, G, H) so **pBasalMeta**=3/8=0.375, but there are four species that have no prey in
836 the local food-web (E, F, G, H) so **pBasal**=4/8=0.5. By comparing proportions of basal and
837 proportions of apex species between two sets of networks, we can also deduce the variation of
838 proportion of mesopredator species.

839 Connectance: We computed the directed connectance of the local network as the average
840 number of prey per species (i.e. the average in-degree, reflecting trophic generalism) divided by
841 species richness, called **dirCon**. This metric captures the density of trophic interactions in the
842 local network and enables to compare the level of generalism independently of richness. We
843 preferred it to the actual average in-degree which tends to scale linearly with species richness
844 and may thus bias our signal here as observed richness is partially biased by heterogeneous
845 sampling effort. Note that we only accounted here for predation on terrestrial vertebrates as we
846 lack data for assessing the full trophic generalism on non-tetrapod species (e.g. invertebrates,
847 marine vertebrates, plants, fungi).

848 Omnivory levels: We computed two metrics for each local network. **omniLvl** takes the average,
849 over locally present mesopredator species in the metaweb (non-basal nor apex), of the standard
850 deviation of their prey trophic levels in the metaweb. This metric is based on a continuous view
851 of omnivory. In the example local food-web of **Figure S4.5**, the mesopredator species are E, C
852 and D. For each of these species, we must gather the trophic levels of its prey in the metaweb
853 and compute their standard deviation (which can't be done from the information available in this
854 virtual example). **omniLvl** is then the average of these three standard deviations. **omniProp**
855 computes the proportion of locally present mesopredator species in the metaweb (non-basal nor
856 apex) that are classified as omnivores, namely feeding on several trophic level intervals in the
857 metaweb. We considered three trophic level intervals: basal (0 to the maximum trophic level of

858 basal species in the metaweb, i.e. 1.572), mesopredators (from the latter to the apex trophic
859 level threshold, explained above), and apex (above the apex trophic level threshold). In the
860 example local food-web of **Figure S4.5**, This definition enables us to locally detect surpluses of
861 species that have a potentially broader trophic niche, even though many of their prey are not
862 locally present. As defined here, our omnivory metrics are insensitive to species richness, basal
863 and apex proportions in the local community. Our choice to exclude apex predators from the
864 computation of omnivory levels is a consequence of the fact that most tetrapod apex predators
865 are very omnivore so that including them would induce a strong correlation with apex proportion
866 and carry no information about the omnivory of mesopredators, which are the main focus of this
867 facet.

868 Chain indices: For each local network, we computed the longest, the mean, and the standard
869 deviation of trophic chain lengths linking basal and top species, based on directed shortest-path
870 lengths. More precisely, we computed the matrix of shortest-path lengths between basal and top
871 species only. Each row of this matrix corresponds to a basal species (no prey in local network),
872 each column to a top species (no predator in local network) and the coefficient (i,j) indicates the
873 length of the shortest path in the network (trophic chain) starting from basal species i and going
874 to top species j. When no path exists from i to j, it is indicated by an infinite coefficient. Note that
875 species without any prey or predator are excluded. Then, we turned this matrix to a vector,
876 removing infinite coefficients, and summarized it with its maximum (**maxPath**), mean
877 (**meanPath**) and standard deviation (**sdPath**) values. For instance, in the example local food-
878 web of Figure S4.5, there are four existing paths from the four local basal species (E, F, G, H) to
879 the single local top predator A. The associated four shortest-path lengths are: 2 (E->A), 2 (F-
880 >A), 3 (G->A), 3 (H->A). Then, maxPath is the largest (3), meanPath is their mean (2.5) and
881 sdPath is their standard deviation (~0.577).

882 Compartmentalization: We hypothesized that the replacement of trophic specialists with trophic
883 generalists and omnivores would tend to break up compartments within networks, i.e. sets of
884 species with denser interactions between them than with the rest of the network. It should
885 translate into a decrease of network modularity (Newman et al., 2006), and a decrease of mean
886 distance between species in the **undirected network** (where the initial directed edges are
887 replaced by undirected ones). Thus, we computed those two metrics, respectively called **modul**,
888 **meanShortDist**, in this architectural facet. More precisely, **modul** is the sum (over all pairs of
889 nodes belonging to a same compartment) of the number of edges between two nodes (zero or
890 one here) minus its expectation if edges were placed at random, standardised by the number of

891 edges. There are several ways to detect communities in a network. We first divided the network
 892 into its connected components (sets of nodes between which there exist a path through edges)
 893 and for each of them, we detected communities inside it with the **cluster_spinglass** function of
 894 the igraph R package (spinglass model with simulated annealing, see Reichardt & Bornholdt,
 895 2006), so that the network communities are the union of communities across its connected
 896 components. Then, the exact formula of the modularity Q for a network of **n** nodes and **m** edges
 897 is given below:

$$898 \quad Q = \frac{1}{4m} \sum_{i,j} \text{com}(i,j) \left(A_{ij} - \frac{k_i k_j}{2m} \right)$$

899 Where **k_i** is the degree (number of edges) of node **i**, **A_{ij}** equals one if there is an edge
 900 between **i** and **j** or zero otherwise, and **com(i,j)** equals one if **i** and **j** belong to the same
 901 community or zero otherwise. The modularity of a network lies between -1 and 1, with a value
 902 above zero if nodes inside each community are more connected than expected by chance. This
 903 is the case in the example local food-web of Figure S4.5 which has a modularity of 0.248. The
 904 spinglass algorithm detected three node communities: (E,C,F), (A,B) and (G,D,H). These
 905 communities make sense visually given the topology of the network undirected transform in the
 906 bottom of Figure S4.5.

907 **References:**

908 MacKay, R. S., Johnson, S., & Sansom, B. (2020). How directed is a directed network?. *Royal*
 909 *Society open science*, 7(9), 201138.

910 Maiorano, L., Montemaggiore, A., Ficetola, G. F., O'connor, L., & Thuiller, W. (2020). TETRA-EU
 911 1.0: A species-level trophic metaweb of European tetrapods. *Global Ecology and Biogeography*,
 912 29(9), 1452-1457.

913 Newman, M. E. (2006). Modularity and community structure in networks. *Proceedings of the*
 914 *national academy of sciences*, 103(23), 8577-8582.

915 Reichardt, J., & Bornholdt, S. (2006). Statistical mechanics of community detection. *Physical*
 916 *review E*, 74(1), 016110.

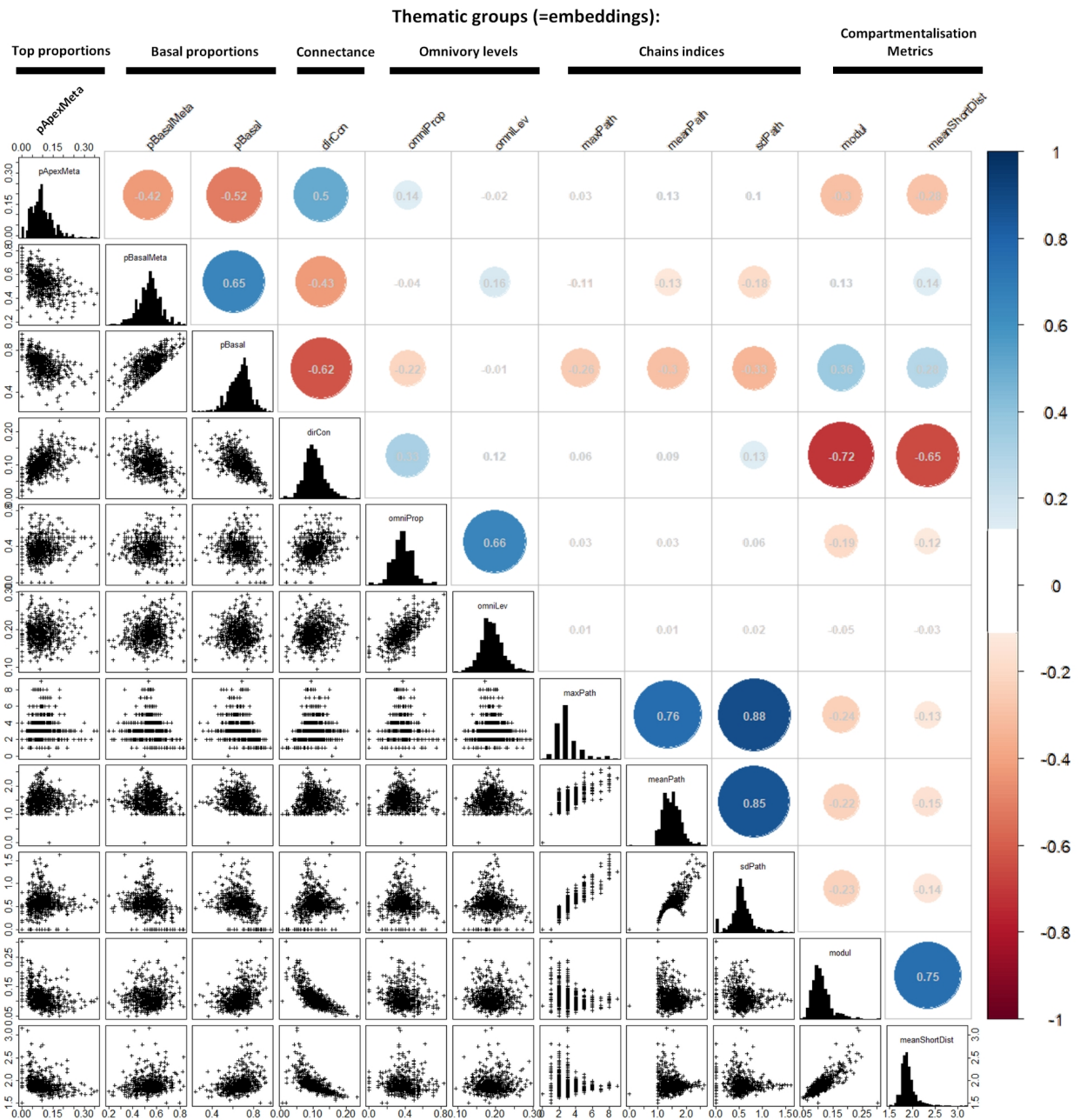
917

918

919 **Appendix S5- Relationships between network metrics**

920

921



922

923 **Figure S5.6.** Relationships between food-web metrics used in this study. Lower triangle: Scatter
 924 plots of metrics values over 650 randomly sampled cells. Upper triangle: Pearson correlations
 925 between metric pairs over all cells.

926

927

928

929

930 **Appendix S6- Quantifying and testing effects of land management intensity**
 931 **on food-webs architecture per land use and bioclimatic region**

932 We notably tested whether the mean deviations related to an increase of intensity were
 933 significant for each facet and context. We tested the equality between the two multivariate
 934 distributions of food-web metrics (high versus low intensity, or medium versus low intensity)
 935 included in the facet, and detected significant deviations when the null hypothesis was rejected
 936 (i.e. no effect of higher land management intensity). This was done using a non-parametric
 937 multivariate test based on Wilk's Lambda statistics, which accounts for the unbalanced number
 938 of cells between intensity levels (Liu et al., 2011, implemented in the *npmv* R package, Burchett
 939 et al., 2017). For every context, we set the first order risk α of detecting at least one false non-
 940 equality across our 6 facets to 5%, which translates into a risk of $1-(1-\alpha)^{1/6} \approx 0.009$ in each
 941 facet, a rather conservative choice. Following the procedure of Burchett et al. (2017), when
 942 three intensity levels were available for a context, we first tested the equality between the three
 943 distributions with risk α , and if equality was rejected, we tested the equality between each pair
 944 with risk $2\alpha/3$, to maintain a strong control of the familywise error rate. The significance of the
 945 deviation in each context is indicated by a blue background of cells in Tables **S6.7** to **S6.11**.
 946

	ATLANTIC	CONTINENTAL	MEDITERRANEAN	ALPINE	BOREAL
medium intensity forest	-0.372	-0.074	+0.009	-0.038	+0.043
high intensity forest	-0.467	-0.126	+0.081	-0.059	+0
medium intensity grassland	-0.101	-0.083	-0.059	-0.346	
high intensity grassland	-0.116	-0.098			
intensive perma. cropland			+0.017		
medium intensity cropland	-0.14	-0.032	+0.146		+0.065
high intensity cropland	-0.192	+0.049	+0.017		-0.129
medium intensity agri. mosaic	+0	+0.048			
high intensity agri. mosaic	-0.045				
medium intensity settlement	-0.014	-0.087	-0.588	-0.437	+0.055
high intensity settlement	-0.024	-0.148	-0.495	-0.487	+0.065

947

948 **Figure S6.7. Food-web metrics deviations related to land management intensity, Part 1: Apex**
 949 **proportion embedding (pApexMeta).** For each bioclimatic region (columns), land use and
 950 land management intensity level (rows), we show the index of variation along each metric
 951 between the considered intensity level (medium/high) and the reference one (low). This index is
 952 the centroid coordinate of the highest intensity group minus the centroid coordinate of the lower
 953 intensity group, divided by the interquartile range of the metric across all studied cells (as in
 954 **Figure 2**). It indicates the direction of the deviation and its importance compared to the dataset
 955 variability. Cells with a number over a white background indicate a significant multivariate

956 deviation in the corresponding context, established with a non-parametric multivariate test, while
 957 cells with a grey background indicate a non-significant deviation and empty cells indicate no
 958 data. A significant deviation is written in pale green when its direction confirms our initial
 959 expectation, in dark red when it contradicts it, and in black for discordant deviations.

	ATLANTIC	CONTINENTAL	MEDITERRANEAN	ALPINE	BOREAL
medium intensity forest	+0.044;-0.073	-0.283;-0.09	+0.175;+0.171	+0.142;+0.014	-0.213;-0.265
high intensity forest	+0.11;-0.033	-0.256;-0.064	+0.465;+0.351	+0.127;-0.24	-0.195;-0.3
medium intensity grassland	-0.217;-0.049	+0.023;+0.093	+0.096;+0.003	+0.013;+0.292	
high intensity grassland	-0.1;-0.069	+0.088;-0.033			
intensive perma. cropland			-0.061;-0.205		
medium intensity cropland	+0.073;+0.076	-0.268;-0.217	-0.325;-0.171		-0.082;-0.228
high intensity cropland	+0.198;+0.153	-0.303;-0.279	-0.479;-0.162		-0.028;-0.111
medium intensity agri. mosaic	-0.205;-0.129	-0.112;-0.024			
high intensity agri. mosaic	+0.032;-0.015				
medium intensity settlement	-0.291;-0.214	-0.041;-0.035	+0.109;+0.195	+0.2;+0.273	+0.049;-0.12
high intensity settlement	-0.312;-0.208	-0.083;+0.012	+0.09;+0.216	-0.049;+0.063	-0.032;-0.126

960
 961 **Figure S6.8.** Food-webs modifications related to land management intensity, **Part 2: Basal**
 962 **proportion facet** (pBasalMeta; pBasal).

	ATLANTIC	CONTINENTAL	MEDITERRANEAN	ALPINE	BOREAL
medium intensity forest	+0.163	+0.14	-0.129	+0.083	+0.17
high intensity forest	+0.23	+0.284	-0.135	+0.245	+0.305
medium intensity grassland	+0.03	+0.094	+0.131	+0.018	
high intensity grassland	+0.039	+0.32			
intensive perma. cropland			+0.117		
medium intensity cropland	-0.152	+0.184	+0.114		+0.29
high intensity cropland	-0.13	+0.296	-0.062		+0.099
medium intensity agri. mosaic	+0.153	+0.043			
high intensity agri. mosaic	+0.155				
medium intensity settlement	+0.039	+0.022	-0.233	-0.329	+0.043
high intensity settlement	+0.081	+0.019	-0.348	-0.315	-0.006

963
 964 **Figure S6.9.** Food-webs modifications related to land management intensity, **Part 3:**
 965 **Connectance embedding** (dirCon).

	ATLANTIC	CONTINENTAL	MEDITERRANEAN	ALPINE	BOREAL
medium intensity forest	-0.025;-0.045	+0.027;-0.036	+0.101;-0.025	+0.183;+0.186	+0.044;-0.053
high intensity forest	+0.131;+0.126	+0.163;+0.058	+0.292;-0.032	+0.45;+0.599	+0.159;-0.009
medium intensity grassland	-0.078;-0.175	-0.053;-0.001	-0.076;+0.126	-0.22;-0.172	
high intensity grassland	-0.077;-0.19	+0.272;+0.079			
intensive perma. cropland			-0.078;-0.004		
medium intensity cropland	+0.133;-0.112	-0.377;-0.298	+0.13;-0.11		+0.2;+0.196
high intensity cropland	+0.125;-0.13	-0.245;-0.214	+0.219;-0.017		+0.15;+0.193
medium intensity agri. mosaic	-0.131;-0.139	-0.085;-0.104			
high intensity agri. mosaic	+0.148;+0.147				
medium intensity settlement	+0.045;-0.029	-0.091;-0.109	-0.105;-0.17	-0.464;-0.218	-0.054;-0.026
high intensity settlement	-0.005;-0.022	-0.172;-0.189	-0.243;-0.326	-0.438;-0.255	-0.116;-0.073

966

967

968

Figure S6.10. Food-webs modifications related to land management intensity, **Part 4: Omnivory levels facet** (omniLev; omniProp).

	ATLANTIC	CONTINENTAL	MEDITERRANEAN	ALPINE	BOREAL
medium intensity forest	-0.046;-0.052;+0.047	+0.148;+0.144;+0.283	-0.084;-0.098;-0.078	-0.05;+0.102;+0.036	+0.292;+0.332;+0.655
high intensity forest	-0.156;-0.149;-0.104	+0.1;+0.064;+0.211	-0.137;-0.117;-0.03	-0.025;+0.207;+0.224	+0.261;+0.308;+0.596
medium intensity grassland	+0.104;+0.075;+0.201	-0.091;-0.063;-0.106	+0.016;+0.042;+0.054	-0.027;-0.161;-0.127	
high intensity grassland	-0.019;-0.01;-0.019	-0.134;-0.072;-0.162			
intensive perma. cropland			+0.1;+0.134;+0.171		
medium intensity cropland	-0.137;-0.191;-0.282	+0.201;+0.27;+0.418	+0.029;-0.021;+0.053		+0.01;-0.003;-0.013
high intensity cropland	-0.17;-0.24;-0.328	+0.005;+0.042;+0.139	+0.063;+0.022;+0.133		+0.019;+0.007;-0.01
medium intensity agri. mosaic	-0.006;-0.06;-0.007	-0.098;-0.135;-0.211			
high intensity agri. mosaic	-0.006;+0.015;-0.016				
medium intensity settlement	+0.017;+0.096;+0.115	+0.054;+0.057;+0.079	+0.002;-0.065;-0.051	+0.029;+0.044;+0.179	+0.284;+0.396;+0.442
high intensity settlement	+0.03;+0.113;+0.142	+0.079;+0.118;+0.145	-0.021;-0.03;-0.053	+0.024;-0.02;+0.015	+0.329;+0.508;+0.595

969

970

971

Figure S6.11. Food-webs modifications related to land management intensity, **Part 5: Chains indices facet** (maxPath; meanPath;sdPath).

	ATLANTIC	CONTINENTAL	MEDITERRANEAN	ALPINE	BOREAL
medium intensity forest	-0.214;-0.02	-0.25;-0.169	+0.129;+0.099	-0.219;-0.049	-0.243;+0.011
high intensity forest	-0.271;-0.085	-0.371;-0.412	+0.305;-0.093	-0.42;+0.018	-0.465;-0.168
medium intensity grassland	-0.007;+0.055	-0.161;-0.161	-0.051;-0.354	+0.016;-0.243	
high intensity grassland	-0.089;+0.004	-0.295;-0.241			
intensive perma. cropland			-0.138;-0.116		
medium intensity cropland	+0.238;+0.371	-0.115;-0.266	-0.056;-0.08		-0.491;-0.509
high intensity cropland	+0.168;+0.312	-0.13;-0.289	+0.208;+0.241		-0.368;-0.347
medium intensity agri. mosaic	-0.026;-0.066	+0.085;-0.013			
high intensity agri. mosaic	+0.017;-0.152				
medium intensity settlement	+0.003;+0.091	-0.116;-0.076	+0.181;+0.363	+0.08;+0.381	-0.21;-0.192
high intensity settlement	-0.061;-0.008	-0.15;-0.07	+0.286;+0.436	+0.141;+0.451	-0.105;-0.104

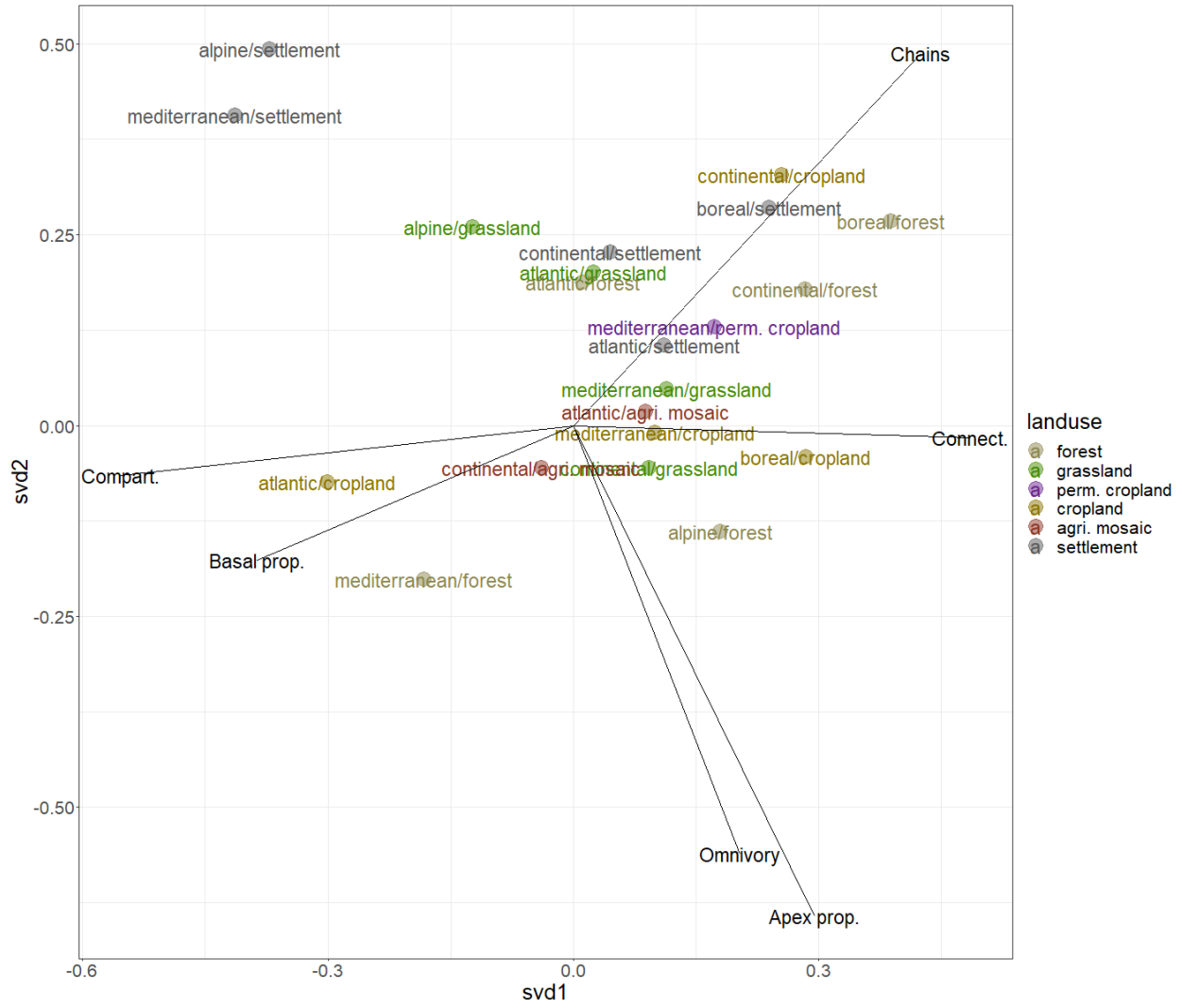
972

973

974

975

Figure S6.12. food-webs modifications related to land management intensity, **Part 6:**
Compartmentalization metrics facet (modul; meanShortDist).



976
 977 **Figure S6.13.** Summary of the relative deviations per context and facet directions in a summary
 978 2 dimensional plane. The multivariate responses of the six facets relative deviations (averaged
 979 for high and mid intensities) over the 21 contexts were summarised in two axes using a Singular
 980 Value Decomposition (SVD), explaining 55% of the total variability.
 981
 982
 983
 984
 985
 986
 987

988 **Appendix S7- Fit of linear models per metric and the relative influence of**
 989 **climate, land use, and land management intensity**

990
991
992
993
994
995
996

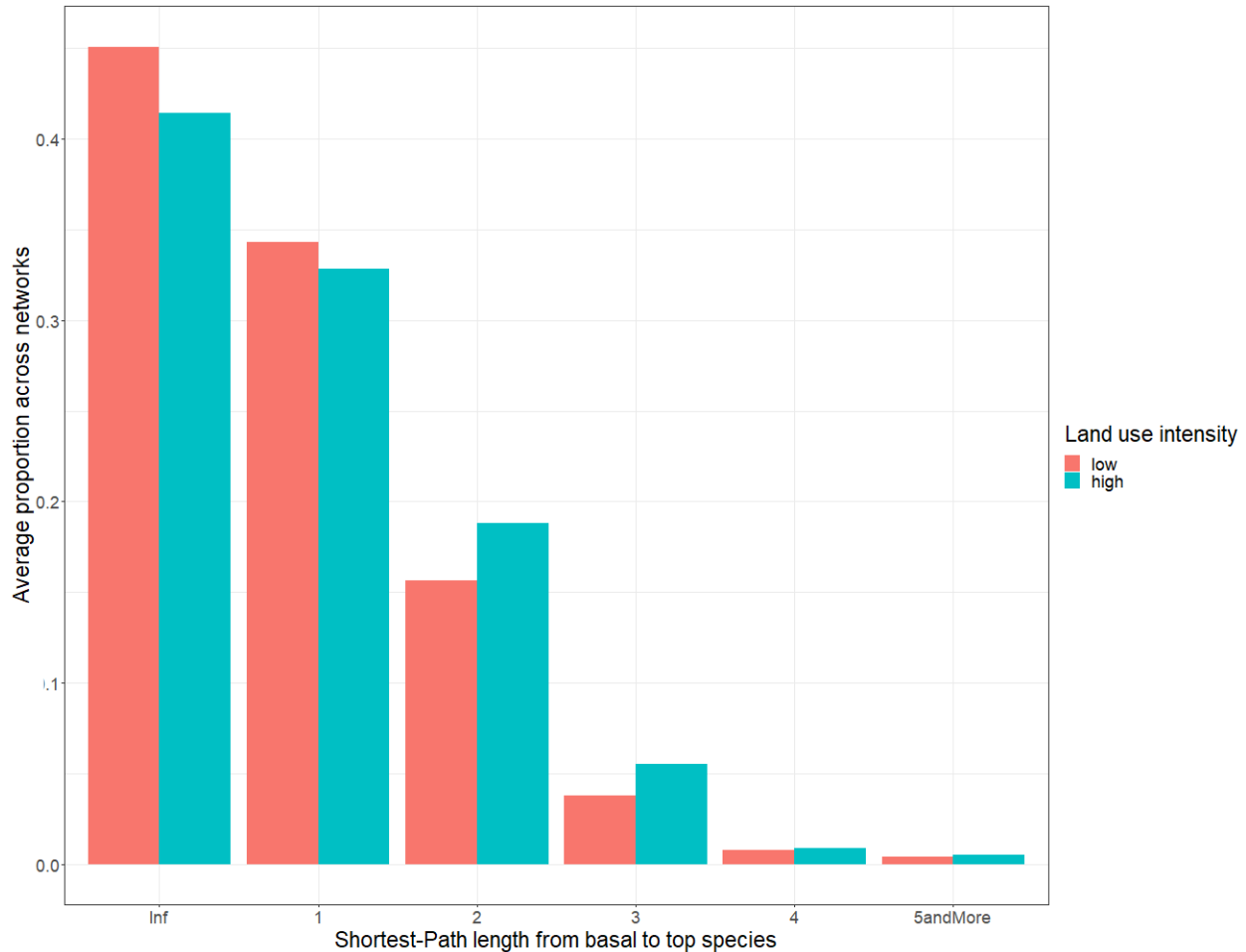
997 **Table S7.3.** Coefficient of determination (R^2) per metric for the full linear model with all
 998 explanatory factors (climate, land use and land management intensity, see column 3) and partial
 999 R^2 s for the sequential addition of the factors: the R^2 with climate only (column 2), and the partial
 1000 R^2 related to the addition of land use (column 3) and to the addition of intensity compared to

Metric	R^2 climate	Part. R^2 Use climate	Part. R^2 intensity use, climate	R^2 all	R^2 (-10% outliers)
pApexMeta	0.163	0.034	0.008	0.198	0.319
pBasalMeta	0.032	0.046	0.007	0.083	0.135
pBasal	0.042	0.032	0.007	0.078	0.131
dirCon	0.009	0.019	0.007	0.034	0.055
omniProp	0.024	0.008	0.004	0.037	0.055
omniLev	0.069	0.025	0.004	0.097	0.161
maxPath	0.015	0.030	0.007	0.052	0.072
meanPath	0.018	0.045	0.009	0.071	0.14
sdPath	0.019	0.030	0.007	0.055	0.072
modul	0.007	0.012	0.009	0.027	0.056
meanShortDist	0.002	0.008	0.004	0.014	0.032
Average	0.036	0.026	0.007	0.068	0.112

1001 climate and land use only (column 4). The full model was also re-fitted (4th column) by
 1002 excluding the 10% most outliers local meta food-webs, namely the 5% most negative and 5%
 1003 most positive residuals.

1004

1005 **Appendix S8- Shortest-Path lengths distribution in low vs high land**
 1006 **management intensity**



1007

1008 **Figure S8.13.** Average proportions of shortest-path lengths from basal to top species in
 1009 European tetrapods food-webs under low (red) or high (blue) land management intensity. We
 1010 used a weighted average to give an equal weight to each bioclimatic region and land use, i.e.
 1011 we averaged proportions over networks in the same bioclimatic region, land use and land
 1012 management intensity, before averaging over all networks in the same land management
 1013 intensity.
 1014

1015 **Appendix S9- Effect of land management intensity on landscape** 1016 **fragmentation and diversity per land use and bioclimatic region**

1017

1018 We computed for each cell three complementary metrics of landscape fragmentation and
 1019 diversity based on the 36km² square window of cells (9x9 cells) centered on the focal cell:
 1020 **patchAntiArea**, **proxToBorder** and **divLandUse**. **patchAntiArea** is the opposite of the number
 1021 of cells contained in the homogeneous patch of land system (land use and management
 1022 intensity) containing the focal cell. **proxToBorder** is the opposite of the euclidean distance (in
 1023 cells) to the closest cell border of this patch. We took the opposite of the last two quantities to
 1024 ensure that an increase of value indicates higher fragmentation. **divLandUse** is the number of
 1025 distinct land system (land use and management intensity) in the 8 adjacent cells to the focal
 1026 one. The mean variation of each fragmentation metric related to higher land management

1027 intensity and the significance of the multivariate deviation are reported per land group in **Figure**
 1028 **S9.14**.

	ATLANTIC	CONTINENTAL	MEDITERRANEAN	ALPINE	BOREAL
medium intensity forest	+4.297;+0.008;+0.438	+8.927;+0.153;+0.244	+17.538;+0.202;+0.591	+16.725;+0.15;+0.757	+0.03;+0.017;+0.215
high intensity forest	-3.742;-0.038;-0.021	-4.378;+0.093;-0.087	+14.011;+0.196;+0.669	+19.688;+0.115;+1.092	-13.593;-0.083;+0.053
medium intensity grassland	-7.735;-0.039;-0.235	-4.638;-0.007;-0.084	+6.102;+0.04;+0.281	+4.603;+0.022;-0.231	
high intensity grassland	-20.038;-0.131;-0.704	-20.301;-0.227;-0.968			
intensive perma. cropland			-5.296;-0.061;-0.207		
medium intensity cropland	-13.167;-0.085;-0.361	-15.126;-0.154;-0.72	-17.607;-0.203;-0.725		-8.957;-0.03;-0.474
high intensity cropland	-20.349;-0.134;-0.551	-7.232;+0.004;-0.277	-4.596;-0.069;-0.358		-0.821;+0.004;-0.114
medium intensity agri. mosaic	-2.918;-0.012;-0.409	-0.704;+0.002;-0.224			
high intensity agri. mosaic	-4.142;+0;-0.318				
medium intensity settlement	-8.373;-0.014;-0.116	-6.621;-0.01;-0.205	-7.076;-0.01;-0.322	-5.337;-0.022;+0.042	-8.227;-0.028;-0.293
high intensity settlement	-24.051;-0.289;-1.069	-18.785;-0.229;-1.127	-14.258;-0.144;-0.891	-3.864;-0.035;+0.025	-7.714;-0.048;-0.68

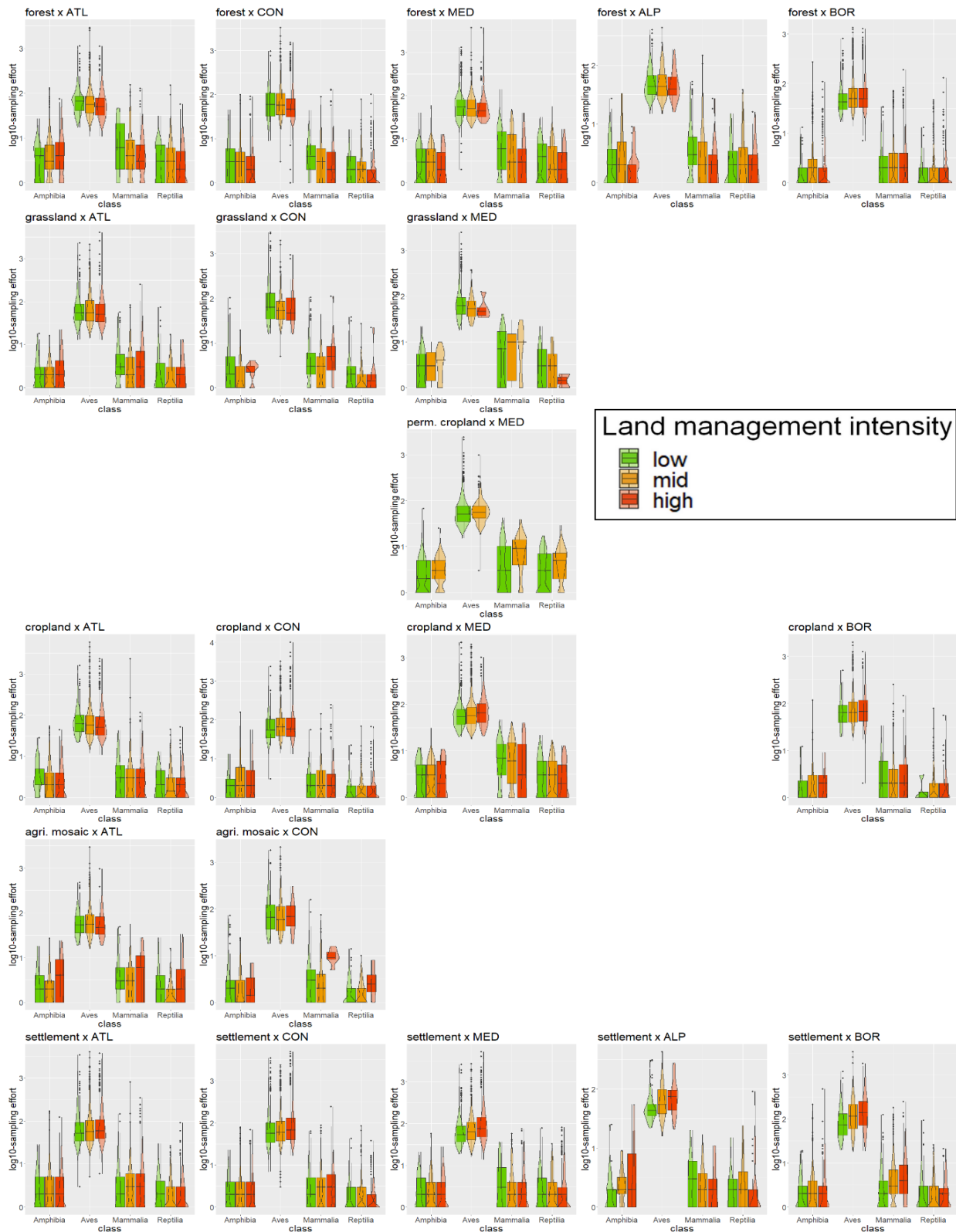
1029
 1030 **Figure S9.14.** Landscape fragmentation and diversity metrics modifications related to land
 1031 management intensity (patchAntiArea; proxToBorder; divLandUse). For each bioclimatic region
 1032 (columns), land use and land management intensity level (rows), we show the mean variation of
 1033 each fragmentation metric related to higher intensity (when taking the low intensity level as
 1034 reference). Cells with a number over a white background indicate a significant multivariate
 1035 deviation in the corresponding context, established with a non-parametric multivariate test, while
 1036 cells with a grey background indicate a non-significant deviation and empty cells indicate no
 1037 data. A significant deviation is written in pale green when positive for the three metrics and dark
 1038 red when negative.

1039

1040 **Appendix S10- Residual sampling effort variations across land** 1041 **management intensity levels**

1042

1043 Our general results arised from the analysis of mean metric deviations related to variations of
 1044 land management intensity for 21 contexts (combinations of land use and bioclimatic region).
 1045 The residual spatial sampling bias can only bias the estimated mean deviation for a given
 1046 context if the sampling effort varies between land management intensity levels. We plot in
 1047 Figure **S10.15** the distribution of log-sampling effort (number of records across cells, the log was
 1048 plotted to visualise to facilitate the comparison across classes) per land management intensity
 1049 (bar colour), taxonomic class (x-axis) and context (plots). The sampling effort varies consistently
 1050 across classes, with birds always showing the highest sampling effort, and among cells per
 1051 context and intensity level, we observe no relationship between land management intensity and
 1052 the median sampling effort, whatever the taxonomic class, except in some rare cases. Hence,
 1053 spatial sampling effort variations should not bias our mean deviation estimates.



1054

1055

1056

Figure S10.15. Sampling effort per taxonomic class, land management intensity for the 21 contexts, namely combinations of land use (row) and bioclimatic regions (column).

1057

1058 Appendix S11- Robustness of general results to various potential biases

1059

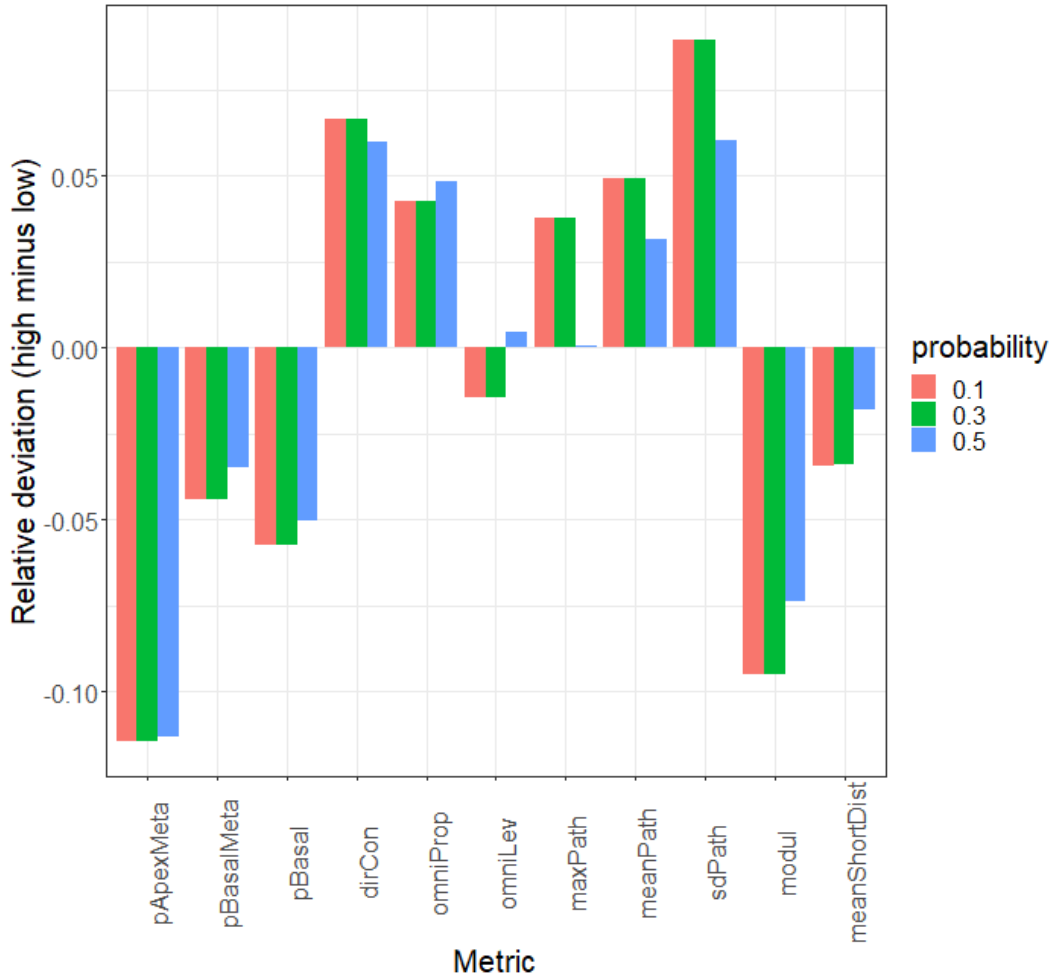
1060 Even though our main analysis was run on the most sampled cells, our cell selection criteria
1061 might potentially allow certain biases to affect our general results. Hence, we carried three
1062 independent sensitivity analyses to test the robustness of our main results to three bias factors:
1063 The stringency of the assumed species detection threshold, the overall sampling bias toward
1064 some taxonomic classes and the outlier food-webs.

1065

1066 For each type of bias, our approach was to subselect smaller set of cells among the 67,051
1067 initially selected cells, where the potential bias is minimised and to measure if our main result
1068 was preserved on this cell subselection, namely the sign and magnitude of the mean deviation
1069 of each metric between high and low intensity cells (as in **Figure 4-top**).

1070

1071 **Sensitivity to the quantile of the detection threshold.** With the cell selection of our main
1072 analysis, the number of species with uncertain absence were generally a small proportion of the
1073 richness per cell, i.e. less than 20% of the observed richness in 84% of cells and less than 10%
1074 in 63% of cells. However, the number of uncertain species in a cell depends on the stringency of
1075 the sampling effort threshold above which a given species is considered truly absent. Hence, we
1076 investigated here the effect of the quantile chosen to generate the species-specific sampling
1077 effort thresholds, determining when the species is assumed absent if not detected. In our
1078 manuscript, we took the first decile (probability=0.1 in **Figure S11.16**) of the sampling effort
1079 values among the species presence cells as the species-specific sampling effort threshold. This
1080 might not be stringent enough to ensure that the species is truly absent for any species. Hence,
1081 we compared here the results obtained when the cell subselection was based on the third decile
1082 (probability=0.3 in **Figure S11.16**) and the median (probability=0.5 in **Figure S11.16**). The
1083 number of selected cells decreased with 64,349 cells remaining when choosing the median. As
1084 a result, the metric deviations are almost unchanged when increasing the quantile, except for
1085 *omniLev* and *maxPath*, for which the deviations collapse. Given that our main results were not
1086 sensitive to the quantile choice, we kept the first decile in our main analysis to maximise our cell
1087 sample size and hence our ability to detect significant deviations of architecture facets in the
1088 weakly sampled contexts (e.g., see Figure).

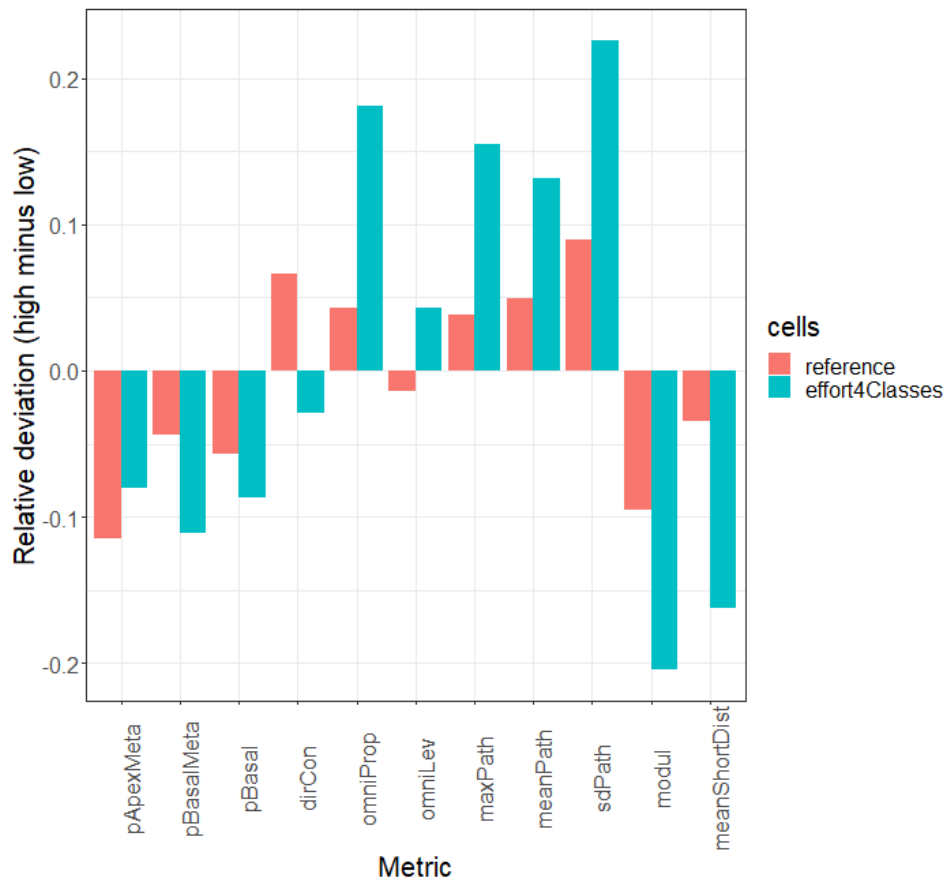


1089
 1090 **Figure S11.16.** Food-web metric deviations related to higher land management intensity per
 1091 architecture facet and per choice of quantile value (0.1, in red, is the reference value of our main
 1092 results), determining the sampling effort needed for any given species to be considered absent
 1093 when not observed. For each metric (x-axis), the mean relative deviation (y-axis) is the average
 1094 of the mean deviation per context of high versus low intensity food-webs divided by the
 1095 interquartile range of the global metric distribution, as in **Figure 4**.

1096
 1097 **Sensitivity to taxonomic bias.** Hence, our network metrics (described below) are likely more
 1098 representative of interaction among birds and mammals, and may hence underestimate the
 1099 effect of other important interactions such as birds preying diverse amphibians and reptiles.

1100
 1101 Birds (Aves) and Mammals were overall much more intensively sampled than other classes
 1102 (Reptilia, Amphibia) in our data, due to the large proportion of crowdsourcing data. Even though
 1103 we imposed that 70% of the 751 tetrapod species must be certainly present or absent for a cell
 1104 to be selected, the 30% remaining species may still concentrate a large part of *Reptilia* and
 1105 *Amphibia* species due to this taxonomic sampling bias. This could potentially affect food-web
 1106 metrics as for instance most *Amphibia* are actually basal species in the metaweb of trophic
 1107 interactions (see **Figure 3**). To minimise this potential bias, we subselected the initially selected
 1108 cells with the constraint that the four taxonomic classes were well sampled. More precisely, we

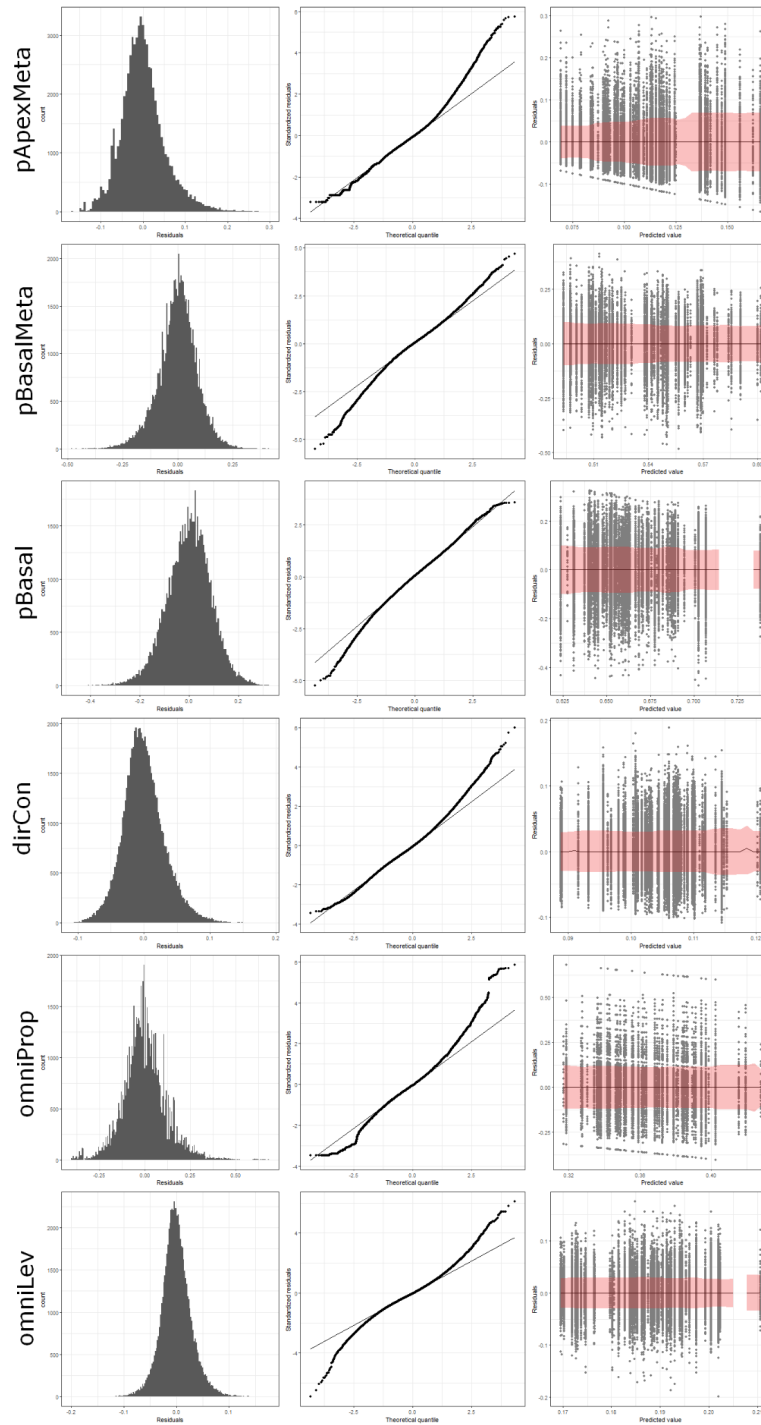
1109 first computed the minimum sampling effort value such that more than 500 cells had a higher
 1110 sampling effort in all four taxonomic classes for both low and high management intensity cells
 1111 (this minimum value was 3). Then, we subselected the associated cells (1329 low intensity and
 1112 561 high intensity cells) and re-computed the 18 mean deviation per metric and compared it
 1113 with our main manuscript result in **Figure S11.17**. It shows that the sign of the deviation is
 1114 unchanged for most metrics, except for dirCon and omniLev.
 1115
 1116



1117
 1118 **Figure S11.17.** Food-web mean relative metric deviations related to higher land management
 1119 intensity per architecture facet for our reference cell selection (red, 67,051 cells) versus a
 1120 subselection with high sampling effort on the four taxonomic classes (blue, 1,890 cells). For
 1121 each metric (x-axis), the mean relative deviation (y-axis) is the average of the mean deviation
 1122 per context of high versus low intensity food-webs divided by the interquartile range of the
 1123 global metric distribution, as in **Figure 4**.
 1124

1125 **Sensitivity to the outlier food-webs.** For each metric, some local food-webs had extreme
 1126 metric values ($|\text{standardised residuals}| > 3$), challenging the gaussian assumption on the
 1127 residuals in linear regressions on the metrics used to estimate their mean deviation per context.
 1128 These outlier food-webs are visible on the quantile-quantile (q-q) plots in the central panel of
 1129 **Figures S11.18 and S11.19**. Most of the q-q plots showed a fat tailed distribution in the
 1130 residuals (except pBasalMeta, pBasal, dirCon), often with a skewness on the right (pApexMeta,

1131 path length and compartmentalisation metrics), mostly due to the 0 lower bound on these
1132 metrics whose value are low in our context. This is not problematic for our significance test on
1133 the multivariate deviation per architecture facet because we tested it using a non-parametric
1134 approach which doesn't rely on the gaussian assumption. However, these outlier food-webs
1135 might potentially bias the deviations in our main results (**Figure 4-top**). Hence, for each food-
1136 web metric, we re-computed the mean relative deviation when removing the outlier food-webs
1137 (in blue in **Figure S11.20**) and compared it to our main results (in red in **Figure S11.20**). Our
1138 main results appear robust to the removal of the outliers responsible for these long tails. Indeed,
1139 for each metric, the mean relative deviations are almost unchanged when removing the outliers
1140 before fitting the linear regression (**Figure S11.20**).
1141



1142

1143

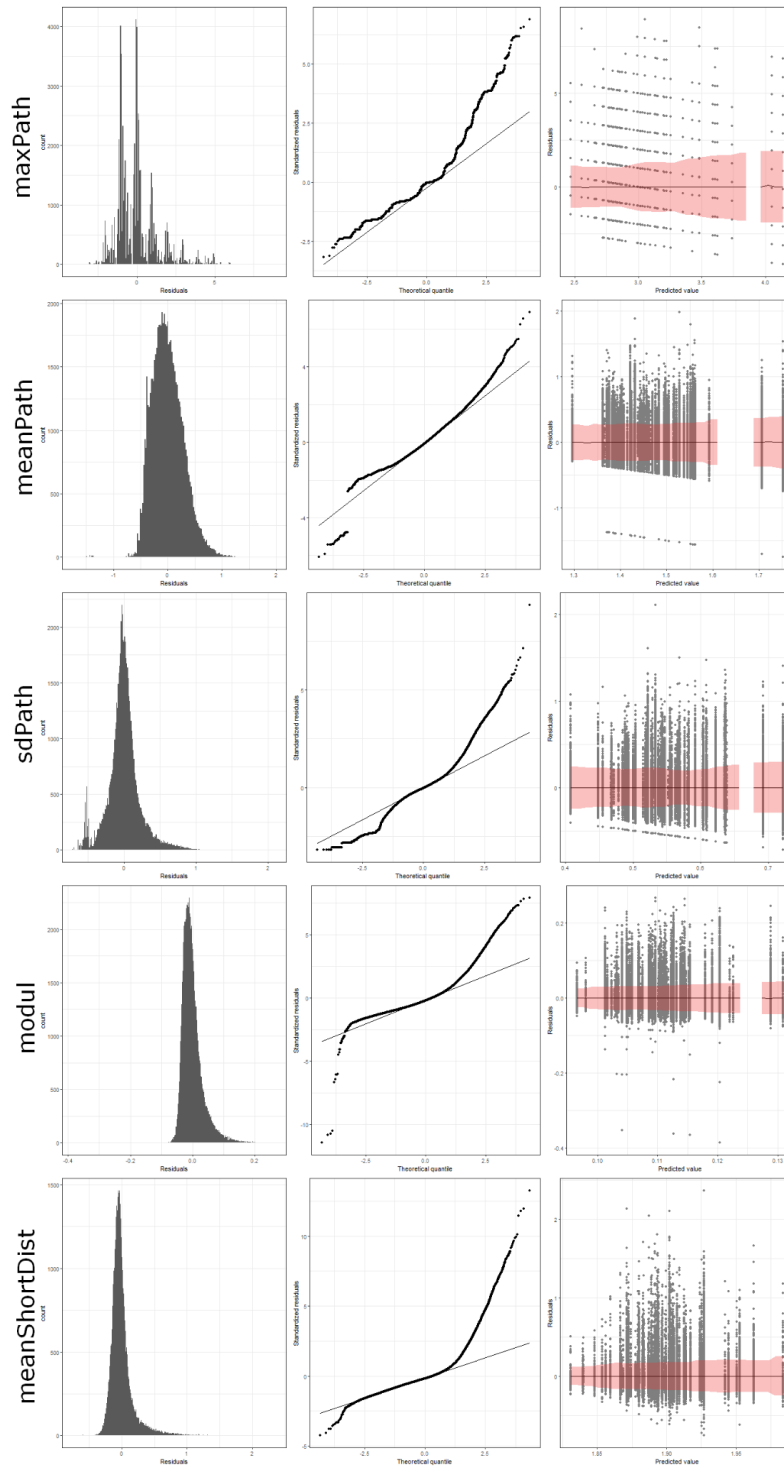
1144 **Figure S11.18.** Part 1 diagnostic plots of the multivariate multiple regression. For each metric

1145 (row), the left panel shows the histogram of residuals, the central panel shows the quantile-

1146 quantile plot to compare the deviation of the residual distribution to a gaussian distribution, and

1147 the right panel shows the mean and standard deviation with a sliding window along the axis of

1147 predicted values, enabling to check for homoscedasticity.

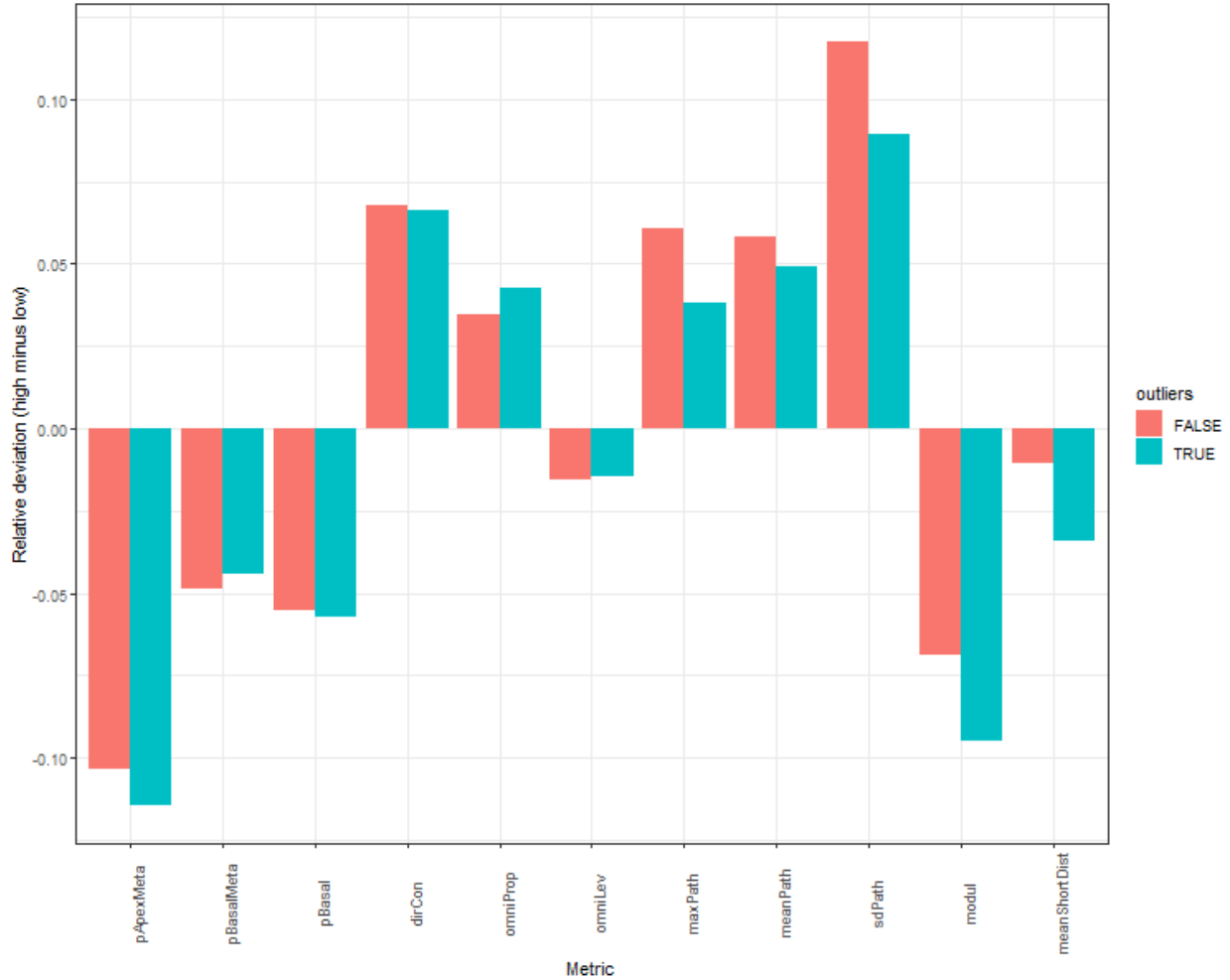


1148

1149 **Figure S11.19.** Part 2 of diagnostic plots of the multivariate multiple regression. Same principle

1150 for the last 5 metrics.

1151



1152

1153 **Figure S11.20.** Food-web metric deviations related to higher land management intensity per
 1154 metric (same as in Figure 4 of main manuscript) for the 67,512 initially studied local food-webs
 1155 including outliers (blue bars) and for the filtered food-webs excluding the outliers of each linear
 1156 regression ($|\text{standardised residuals}| > 3$).